A BEAM SCANNING DEVICE
FOR THE
UNIVERSITY OF MANITOBA
CYCLOTRON FACILITY

BY

CHRISTOPHER HADDOCK

A THESIS

Submitted to the

FACULTY OF GRADUATE STUDIES

In Partial Fulfillment of the Requirements

for the degree

MASTER OF SCIENCE

DEPARTMENT OF PHYSICS

UNIVERSITY OF MANITOBA

WINNIPEG, MANITOBA

A BEAM SCANNING DEVICE
FOR THE
UNIVERSITY OF MANITOBA
CYCLOTRON FACILITY

BY

CHRISTOPHER HADDOCK

A thesis submitted to the Faculty of Graduate Studies of
the University of Manitoba in partial fulfillment of the requirements
of the degree of

MASTER OF SCIENCE

TABLE OF CONTENTS

ABSTRACT

This thesis describes the design and development of a beam scanning device over the period Spetember 1978 to February 1981 at the University of Manitoba 50 MeV cyclotron facility.

A review of the ways of imaging a proton beam is given, followed by design and construction details of a beam scanner.

A scanner now exists which can detect proton beam currents as low as 18 nano-Amperes from the cyclotron exit port and 1 nano-Ampere from the polarized ion source.

The scanner also has a unique feature in that it will give an intensity profile of a beam of low energy neutral particles.

ACKNOWLEDGEMENTS

I would like to thank all members of the technical staff of the Department of Physics most notably Alan McIllwain and Irv Gusdal for helping me set up and "de-bug" the scanner, Richard Hamel for designing and building the electronics and Jim Anderson and Tony Smith for designing the hardware and software respectively in the emittance measurement. All of their help is greatly appreciated.

Thanks too to my supervisor, Francis Konopasek, for his help during the course of my degree.

FIGURE CAPTIONS

CHAPTER 1

INTRODUCTION

INTRODUCTION

For precise alignment and guiding of sub-atomic particles along the beam lines of accelerators a monitor is necessary which gives information about the intensity and position of the beam.

Once beam width, displacement and divergence are known, beam optics can be set to guide as much of the beam as possible from accelerator to experimental area.

The project described in this thesis set out to build a beam scanner - a device which would give a cross-sectional view of the intensity of the charged particle beam and its displacement from the beam tube centre. A review of the various types of scanner that had already been built at various accelerating laboratories was undertaken and it was hoped to design a hybrid unit which would embody the best aspects of the various scanners.

The University of Manitoba cyclotron is a variable energy machine from 28-50 MeV with proton beam currents as high as 5μA. At the present time the cyclotron uses a screen system to image the position of the proton beam. Screens are injected into the line and viewed with a television camera. In the accelerating vault one camera can look at four screens shown in Fig. 1.1 but in the experimental area one camera is needed for each screen. A beam scanner in the position of a screen is cheaper and gives intensity information also.

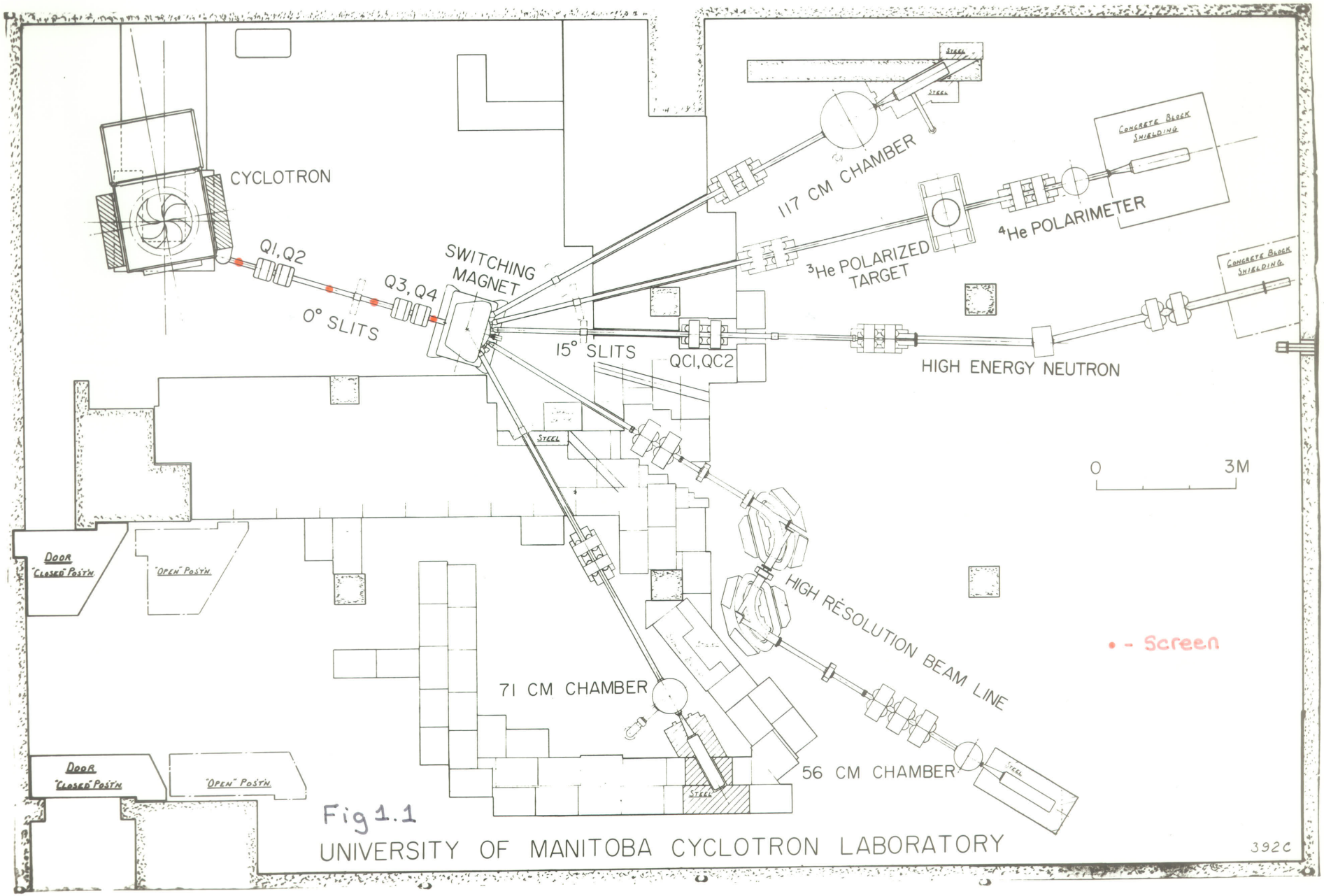

Fig 1.1

UNIVERSITY OF MANITOBA CYCLOTRON LABORATORY

A beam scanner has been developed which will monitor a 3mm wide beam down to 18 nano-Amperes and which can give an intensity profile of neutral particles. The estimated cost of construction and materials is $150.00 by Physics Department machine shop technicians, while a similar commercially available unit is quoted at $1,700.00. The basic criteria to be fulfilled by the scanner were:

(i) A real time output.

(ii) Negligible distortion on the particle beam.

(iii) Low cost.

(iv) Easy to maintain.

(v) Intensity profile as well as beam position output.

These factors are described in the chapters that follow together with a description of how the beam scanner built is incorporated into an emittance measuring device to measure the emittance of the beam from the cyclotron.

CHAPTER 2

DESIGN CONSIDERATIONS

SECTION I. A review of the types of scanners.

SECTION II. Secondary electron emission.

INTRODUCTION

Many types of beam scanner have been built, from simple photographic emulsions to complicated multi-motorised driven units. These have been described fully in the scientific literature.

It was proposed to study the various ways of obtaining information about an accelerated proton beam and to build a hybrid unit which would embody the best features of the different types of scanner.

A literature search was done and this chapter gives a review of the types of beam scanner, and a discussion of the reasons the scanner described in chapters four and five was designed.

The scanner designed works by utilizing the principle of secondary electron emission. Some of the aspects of this emission are described in Section II.

SECTION I. - A Review of the types of beam scanner.

There are many types of scanner and each has its own peculiarities but they fall into three basic categories:

(i) Non-intercepting types.

(ii) Those which stop or disturb the beam.

(iii) Intercepting types in which beam disturbance is negligibly low.

These will be discussed below.

(i) Non-Intercepting Types

Using magnetic induction techniques, a non-intercepting device finds the time average position of the beam at the Argonne National Laboratory cyclotron.[1] Two sets of detection coils determine the horizontal and vertical positions of the beam. Each set consists of two coils connected in opposition and symmetrically placed about the mechanical centre of the beam tube. The axes of the coils are located perpendicular to the direction of propagation of the beam. The coils are resonantly tuned to the frequency of the beam bursts from the cyclotron. The voltage induced per coil is given by:

$$e = \frac{K}{r} \frac{di}{dt}$$

where $i(t)$ -is the beam current.

r -is the effective distance from current filament to coil axis.

t - time

K - a constant

The magnitude and polarity of the induced voltage 'e' thus give the displacement of the beam and for two coils connected in opposition the voltage output would be zero for a beam at the centre of the beam tube. The detector can locate a beam current of 30 nano-Amperes with a positioning accuracy of 0.1mm with positioning accuracy decreasing for lower beam currents. However, this particular scanner gives no information on beam profile.

(ii) Types which Disturb or Stop the Beam

These types can be subdivided into those types which give beam profile or displacement measurement while the accelerating machine is running and those which require off-line analysis of an irradiated material as discussed below.

When a scintillating screen is placed in the beam, the rough dimensions of the beam can be seen as it strikes the screen. This is the system presently used at the University of Manitoba cyclotron, screens are inserted into the line via compressed air. In the accelerating vault a television camera looks at the desired screen by reflection in a mirror. The screens show displacement of the beam from the centre of the beam tube but again do not give a beam profile. When a screen is used the beam delivered to

the experimental area is interrupted.

At the Stanford Linear accelerator,[2] a 1mm square molybdenum target is moved through the beam. The scattered beam produces an electromagnetic shower down the accelerator structure which is measured by a nearby ionization chamber. The resulting intensity gives a beam profile as the target is driven by motors in a Lissajous type figure of about 2.5 square centimeters. A complete scan takes approximately 20 seconds.

A further type used at the Radiation Centre of Osaka[3] monitors the profile of a beam as it leaves the exit window of a scanning linear accelerator. Some electrons are scattered through large angles as they leave the window; however, the beam profile of these electrons remains same. An array of thirty copper sensors is mounted at 40° around the exit window, the current produced by each of these is amplified and fed to a readout to display the beam profile.

The three types of monitor mentioned above operate when the accelerator is running. Other types will give a profile by examining a piece of material after it has been irradiated. An example of this is the irradiation of gold foil.[4] When bombarded with protons the foil becomes an X-ray source. After removal from the accelerator structure the foil is placed in contact with X-ray sensitive film. The developed film is scanned with an optical densitometer and

the output intensity from the densitometer results in a beam profile.

In similar ways, ^{149}Terbium, an α particle emitter produced again by the irradiation of gold is scanned with an α detector and an array of γ ray active aluminium rods is scanned with a γ ray spectrometer to give intensity profiles which are the same as the cross-sectional intensity profile of the particle beam.

As a final example of this type of scanning method, thermoluminescent sheets when heated after irradiation give a light output across the sheet proportional to the intensity of the beam at each point.[5]

(iii) Intercepting Types

With these types of scanner the disturbance of the beam is negligibly low so that profiles may be observed as beam optics are changed without interrupting the beam incident on the target.

All of these types work by placing or passing a single wire or an array of wires through the beam. Secondary electron currents produced as the beam strikes these wires are amplified and read out to give position and profile data. The monitors fall into the subdivisions described below.

(a) Grids

Here a grid of wires is wound on a former in horizontal

and vertical directions.[6,7] Each wire is insulated and the current produced in each wire as the beam strikes it is read out to give a histogram type profile. The grid of wires is injected into the beam line in much the same way as the screen system described above. The grid is removed when not in use to reduce heating of the wires.

(b) Plane Scanners

In an example of this type of scanner a single wire driven by a motor and pully system traces out an X-Y plane perpendicular to the direction of propagation of the cyclotron beam.[8] The wire moves in the X direction and the slowly changing current produced by the incident beam is amplified and recorded on a chart recorder or storage oscilloscope. When the X direction profile has been produced, a microswitch is activated to produce the Y profile. Another type used at the Oxford Tandem accelerator[9] uses a wire bent into a pentagon-like shape. Pivoted at one point, the wire vibrates rapidly through the beam. It is shaped in such a way that it gives the X and Y profiles on each passage through. The speed of the vibrations eliminates the need for a storage oscilloscope as used above, an ordinary oscilloscope will display the profile.

(c) Cylindrical Surface Scanners

These scanners form the bulk of beam scanners used at accelerator laboratories and are the only type of scanner

manufactured commercially. They consist basically of a wire attached to an arm on a rotor. They scan on the surface of a cylinder the axis of which is perpendicular to the direction of propagation of the beam. Differences arise in the type of motor used to drive the scanner, for example a phase sensitive motor giving a real time output[10,11] or a stepping motor driven scanner giving a chart recorder, oscilloscope or computer graphics output.[12]

DISCUSSION OF SCANNERS

From the outset the criteria for the scanner were:

(i) To build a scanner that would give a real time output.

(ii) A scanner that would not interfere with or disturb the beam.

(iii) One that was as simple as possible to reduce maintainance.

(iv) Low cost.

(v) Must be able to give profile as well as displacement.

The monitors which stopped the beam were thus ruled out, so too was any type of scanner which required a storage oscilloscope such as a stepping motor driven wire scanner or a grid of wires. The final decision was between wire monitors which scanned on a plane and those which scanned on the surface of

a cylinder.

The plane scanners have a "whipping" effect at the end of each scan and this can lead to a distorted beam profile indicating more or less intensity at a particular point on the plane of the resulting display.

The cylindrical surface scanners have two distortion effects. (a) The projection of the position of the wire onto a diameter of the circle in which it is moving gives simple harmonic motion rather than a linear motion, oscilloscope scanning is usually linear and this would result in some distortion of the observed profile. (b) The second distortion is that the scanner measures the intensity not on a plane but on the arc of a circle, thus there is an out of plane distortion which again affects the display.

SCANNER CHOSEN

Despite the two distortions mentioned above, a cylindrical surface scanner was chosen. The out of plane distortion is negligible for beam transport systems with focal lengths > 1.0m. The first distortion mentioned above has been overcome as described in Chapter 2 on the prototype scanner.

SECTION II. Secondary Electron Emission

Many types of beam scanner including the one described here rely on secondary electron emission to give a profile of a charged particle beam. The number of secondary electrons released as a wire passes through a proton beam is proportional to the intensity of the beam at every instant.

When the secondary electron current produced is collected and amplified for display, a cross sectional intensity profile of the beam results.

It is surprising that scanners using this technique work so well since, as described by Beck[13] the secondary electron emission efficiency given by:

$$\gamma = \frac{N_e}{N_i}$$

where N_e - is the number of secondary electrons produced

N_i - is the number of incident particles

is only a few percent when the incident particle are 50 MeV protons. The mechanism of secondary electron emission is described by Sternglass.[14] The most interesting and surprising finding is that the secondary electron emission efficiency does not depend on the work function, conductivity, or crystal structure of the metal used but is roughly constant at a particular energy of incident particle. Only secondary electrons produced near the surface i.e. within 10^{-8} to 10^{-9}m

can escape from the wire and they leave with energies of 6-8 eV. The yield of these electrons is proportional to the energy loss of the incident particle. Since in wire scanners the wire has a negligible effect on the charged particle beam, the yield at 50 MeV is low. At lower energies the yield increases and is a maximum in the KeV range. These are the energies encountered in the ion source and as described in Chapter 5 the scanner output can be fed directly to an oscilloscope without amplification, since the secondary electron current is much higher.

For metals of low atomic number such as Beryllium and Lithium, an oxide coating increases the secondary electron yield and it has been found[15] that the increase continues with time of outgassing towards a limiting value many times the original yield.

For higher atomic number metals with an oxide coating the yield of secondary electrons decreases with time of bombardment and outgassing to that of a clean metal surface.[15]

In the scanner described in the next Chapter, steel, nickel-chrome and thoriated tungsten wires were tried as scanning wires. The size of the output signals was the same so steel was used for convenience.

CHAPTER 3

THE PROTOTYPE SCANNER

INTRODUCTION

As said in the design considerations, a rotating wire scanner was to be designed for the University cyclotron. This chapter describes mechanical and electronic details of the scanner, followed by modifications made as the development progressed.

Also discussed are the noise sources present and how they were reduced to a minimum.

I. MECHANICAL DETAILS

The design for the prototype scanner initially followed that of Bond and Gordon.[16] The scanner is shown in schematic form in Fig. 3.1.

A double shafted motor forms the heart of the scanner. The upper shaft carries the rotating arm to which the 1.0mm diameter steel scanning wire is attached, while the lower shaft carries an optical shaft position encoding device. The output of the shaft encoder gives information on the position of the wire in the beam tube.

(a) Motor

Since the motor was to operate inside the vacuum system a search of the motor literature was done to find the motor most suitable. This turned out to be a Singer-Kearfott company CT20173002 synchronous motor which had been tested at low pressures. However, the price for this motor was quoted at $340.00 each. To keep the price of the scanner as low as possible, tests were performed on a double shafted Electrohome SM418 motor similar to that found in small fans.

The motor in the scanner would operate only intermittently in use, however to see if heating of the motor would be a problem it was run in a vacuum of a few hundred microns for half an hour. The only cooling was by contact of the motor

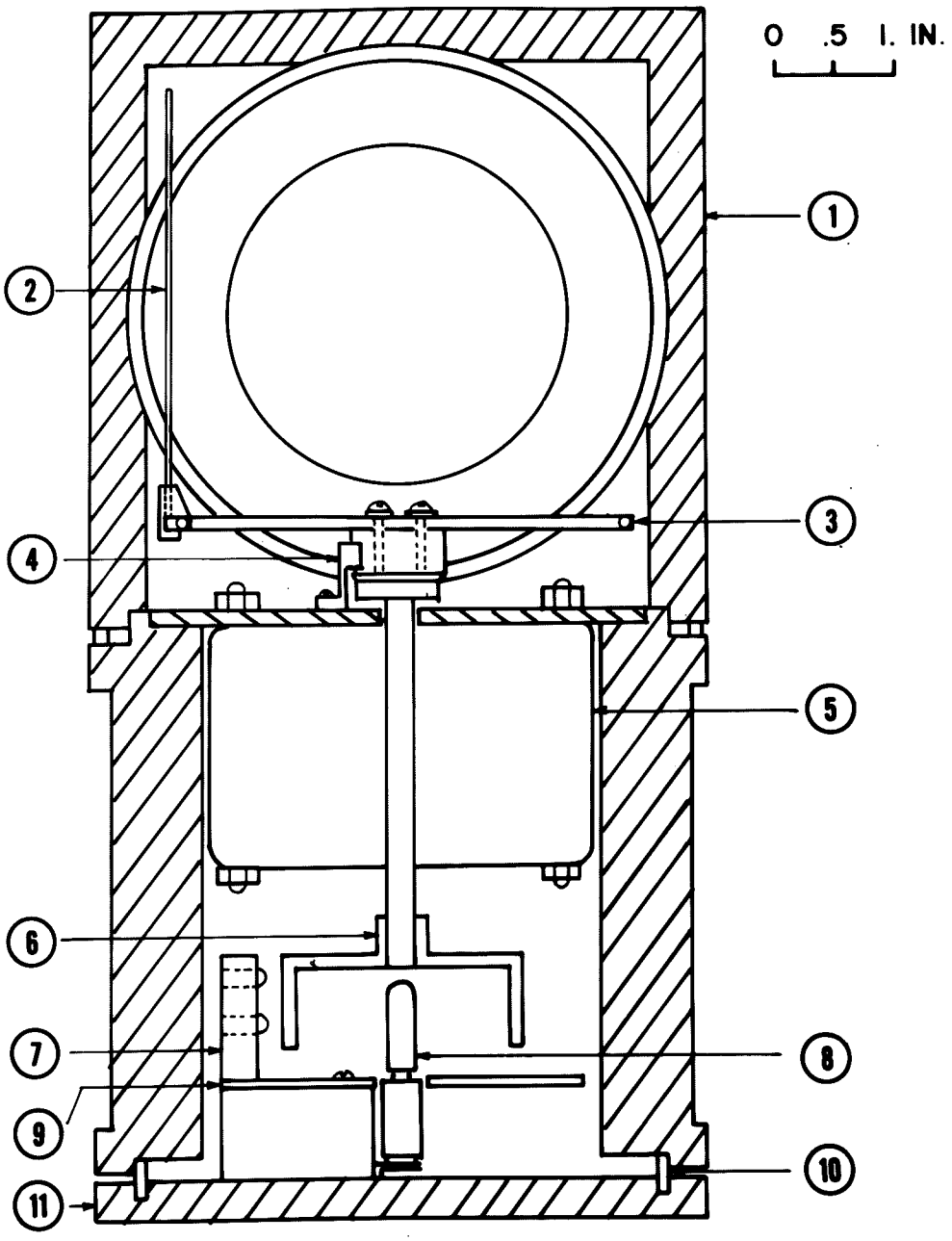

.1 Prototype Scanner
matic.
andard 4" bean cube
anning wire
anning bar

4) Secondary electron pickup
5) Motor
6) Cylindrical encoder
7) Phototransistor assembly
8) Light source
9) Light baffle
10) 'O'ring vacuum seal
11) Base plate

with the floor of the vacuum chamber. The temperature of the motor reached 150° centigrade, only a few degrees higher than that obtained by running the motor in air for a similar period of time.

It was felt therefore that the only problem that would be encountered would be the outgassing of the lubrication of the shaft, this was to be solved by using nylon sleeve bearings. In fact over the time that the first scanner was used no problems with the motor bearings were encountered at all.

(b) Scanning bar and pickup

The prototype scanner used a brass rotating bar nine centimetres long with a hinged end. A spring would pull the wire out of the beam when the scanner was not being used. When the scanner was switched on, centrifugal force would lift the wire into an upright position. This is described further in the alignment of the scanner. A rotating contact made from phosphor-bronze formed the current pickup. Secondary electrons released from the wire result in an amplifier input current which is fed back down through the scanner housing to the input of the beam profile amplifier.

(c) Scanner housing

The scanner housing was made from aluminium except the base which was made from brass for easier welding. An

auxiliary pumping port for the vacuum system was welded to the base plate but it was never needed since pumping of the scanner housing from the beam line was sufficient. The port was not included on further scanners. The scanner housing scanning bar and current pickup are shown in Fig. 3.2.

(d) Shaft encoding arrangement

A light "chopping" arrangement was used to encode the position of the shaft. A cylindrical drum was attached to the lower shaft of the motor, this drum was cut out in such a way that it would block light from a small 6 volt d.c. bulb to a pair of MRD-450 phototransistors for part of a revolution of the shaft. One phototransistor would be illuminated for half a revolution and blocked for the other half, giving rise to a square waveform output with the same frequency as the rotational frequency of the motor. The other phototransistor would be illuminated for only a fraction of a revolution giving rise to a 200μ second width pulse once every revolution of the motor. These outputs were used for shaft position and scanner alignment. The light encoding arrangement is shown in Fig. 3.3 where one can see the mounted phototransistors and cut-away drum.

(e) Alignment

The light encoding device gave outputs as shown in Fig. 3.4. If the oscilloscope controls are adjusted so that

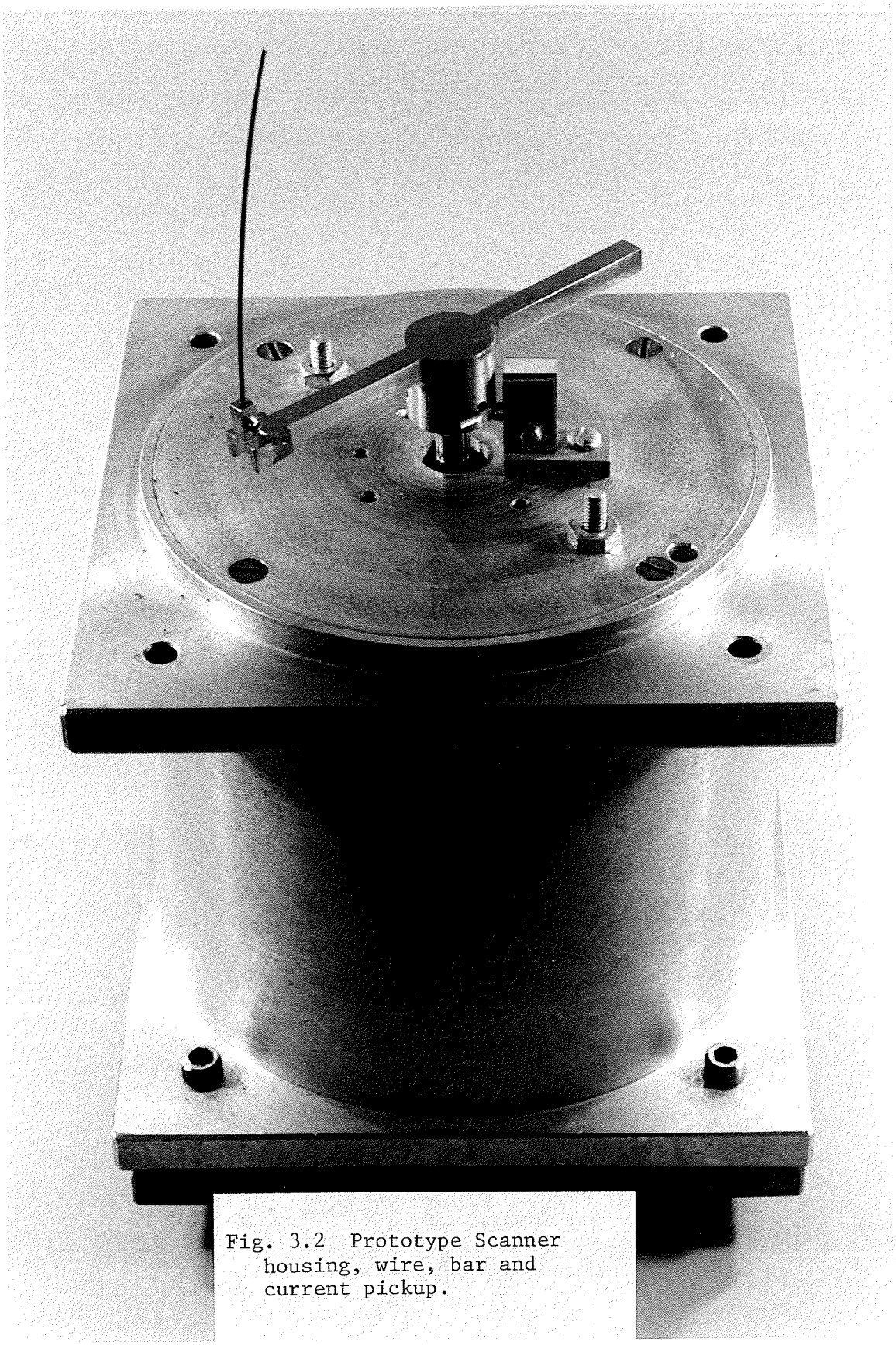

Fig. 3.2 Prototype Scanner housing, wire, bar and current pickup.

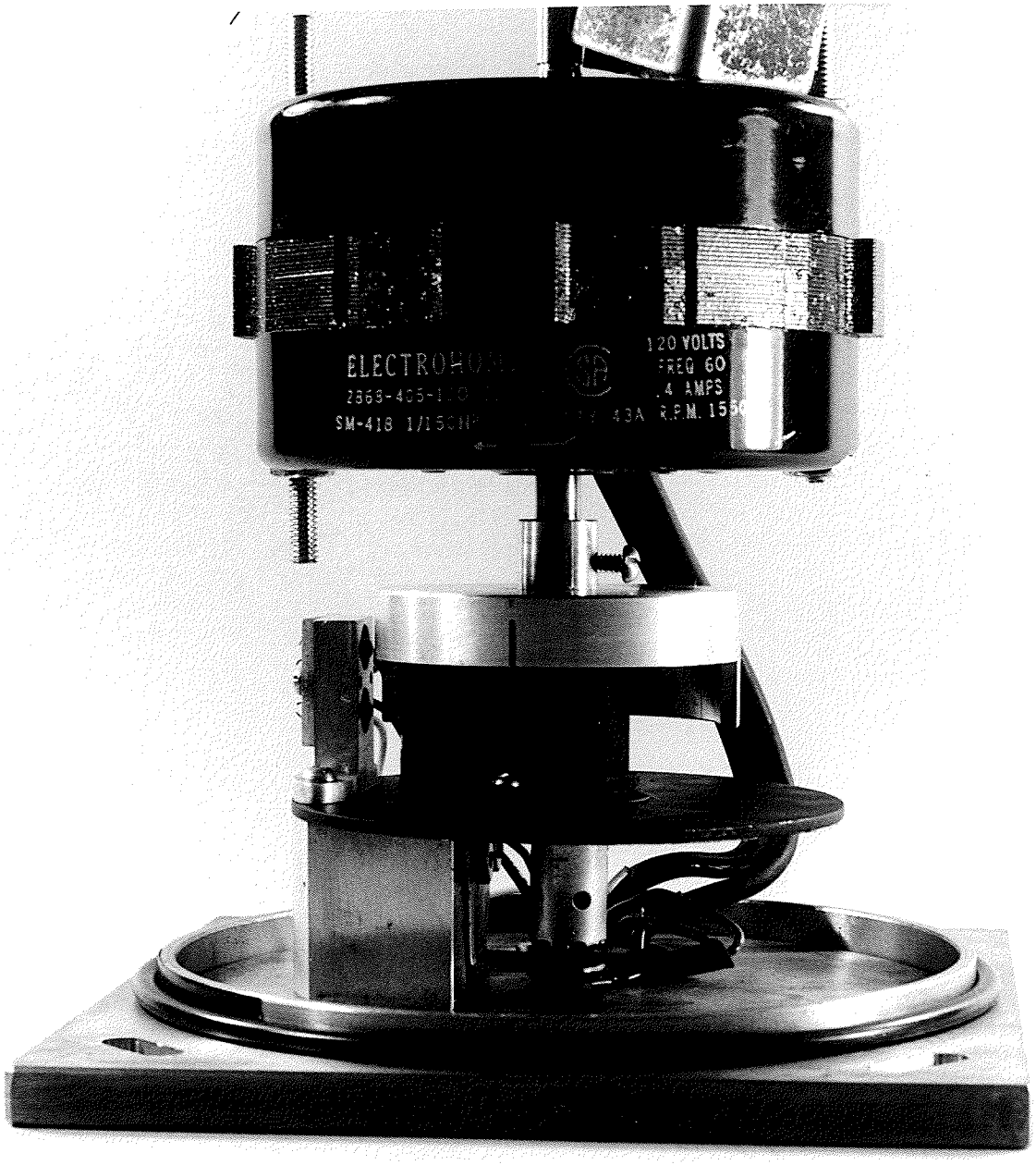

Fig. 3.3 Light encoding arrangement inside scanner.

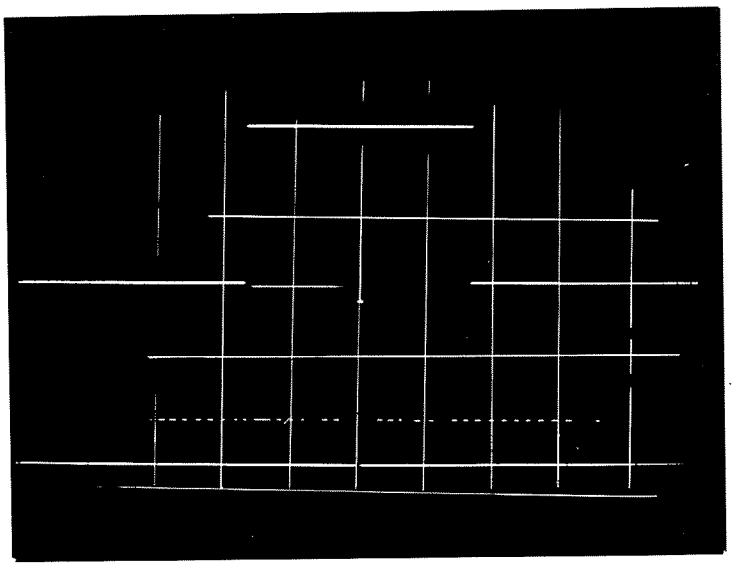

Fig.3.4 oscilloscope outputs of the light encoding device

the length of the positive half of the square wave is the length of the scanning bar, then one has a measure of the beam width and displacement. The pulse (lower trace Fig. 3.4) is used to trigger a stroboscope which illuminates the position of the wire when the pulse is produced. By adjusting the bar on the shaft the position of the wire can be made to coincide with the centre of the beam tube as the pulse is produced. Thus the pulse output represents the centre of the beam tube. When this is done the pulse output can be used to trace brighten the profile display, showing the centre of the beam tube as a bright dot on the profile.

The pulse output also serves to check the shape of the wire when it is in the scanning position. Figs. 3.5 and 3.6 show the strobed illumination of the wire as it rotates. Fig. 3.5 show that when the light encoding arrangement is aligned properly, the scanner wire is at the centre of the beam tube as the pulse is produced. Fig. 3.6 shows that after suitable forming of the wire it is straight when the scanner is running. This is important if an accurate cross sectional profile is to be obtained. A general view of the strobed lighting is shown in Fig. 3.7.

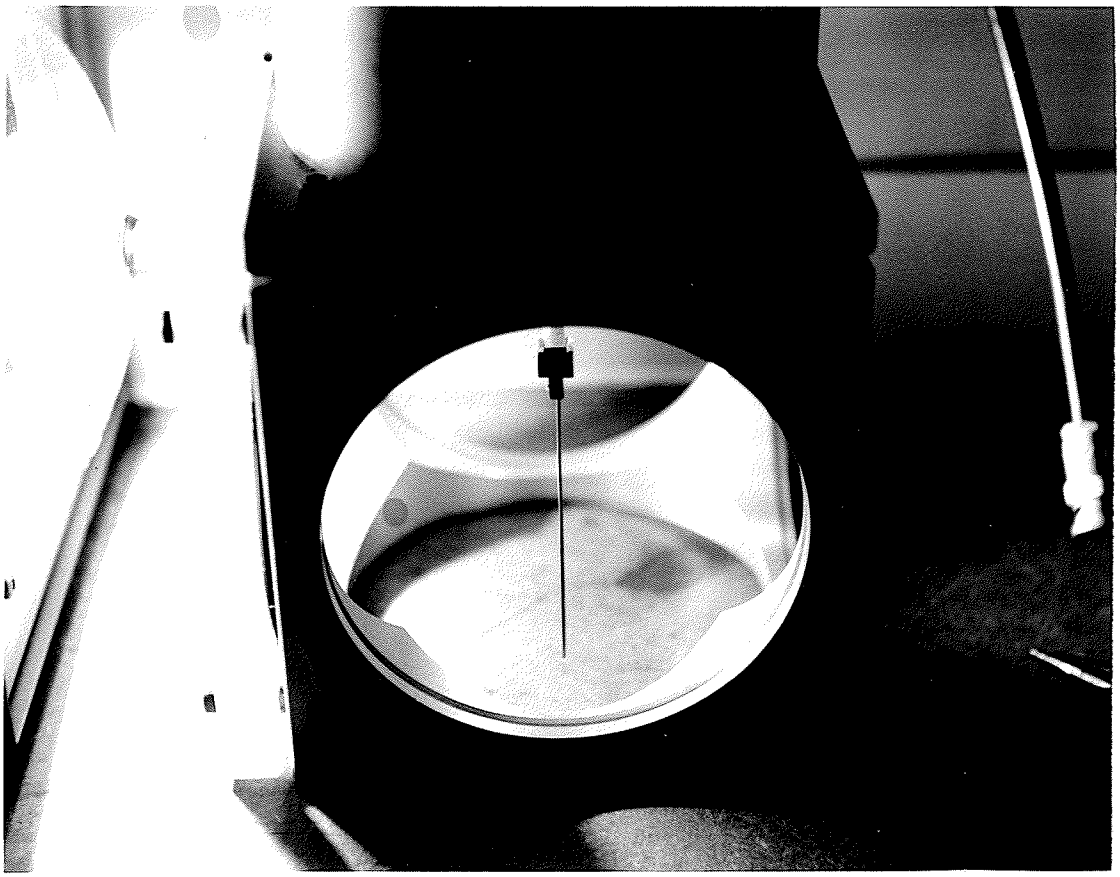

Fig. 3.5 Strobed illumination of Scanner wire aligned at centre of beam tube.

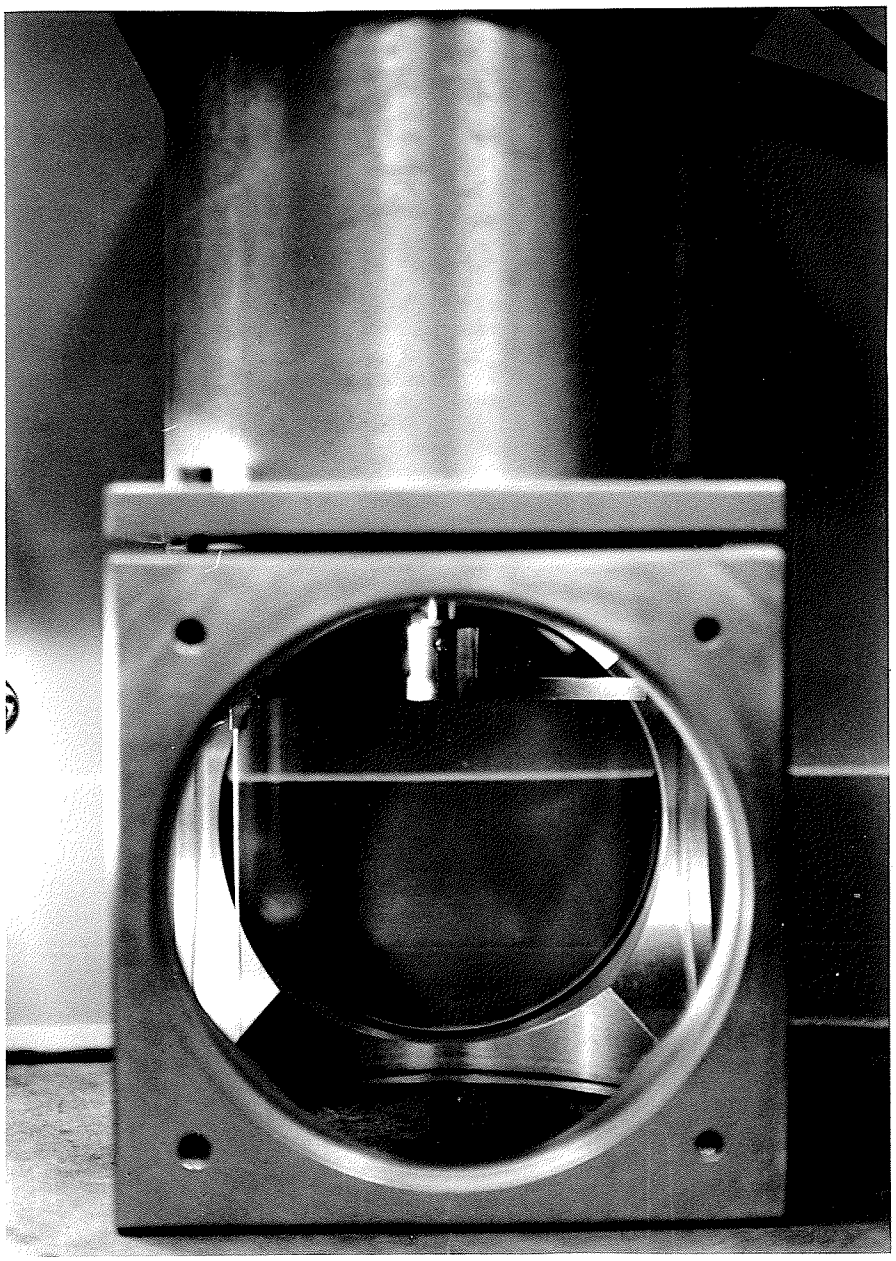

Fig. 3.6 Strobed illumination of the rotating wire shows that it is straight when the scanner is running.

Fig. 3.7 General view of strobed lighting.

II. ELECTRONICS

This section gives details of the electronics associated with the prototype scanner. All the outputs from the scanner were amplified in the vault and fed back to the control room for viewing directly on an oscilloscope. The speed of the motor was chosen so that a flicker-free image would be produced on the oscilloscope. The electronics consists of power supplies for amplifiers, bulbs and motors, amplification circuits for phototransistor outputs, a square wave to sine wave converter and a high gain amplifier for the beam profile signal.

(a) Power supplies

As shown in Fig. 3.8 the 117 volt mains supply is transformed down, rectified and passed through voltage regulators to give +12 and -12 volts d.c. supply voltages for the beam profile amplifier and +12 volts d.c. for the phototransistor amplifier circuits. A centre tap on the transformer gives, after rectification, 6 volts d.c. supply to the bulb which illuminates the phototransistors. Two power supplies were built into one rack-mounting housing since in practice scanning in the X and Y directions is required.

(b) Phototransistor circuits

Fig. 3.9 shows the amplification circuit for the MRD 450 phototransistor output. The rise time of the transistor

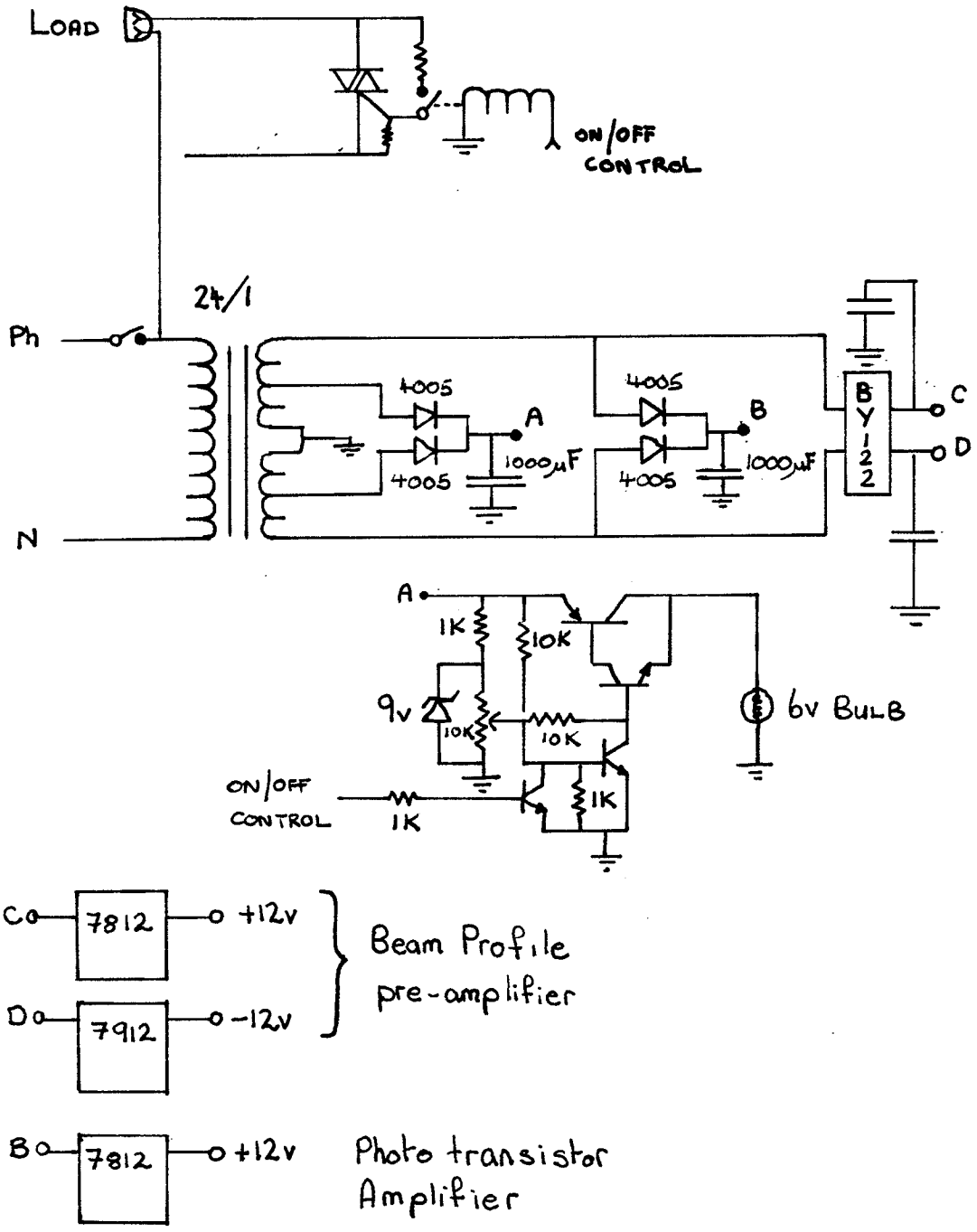

Fig. 3.8 Power Supply Schematic.

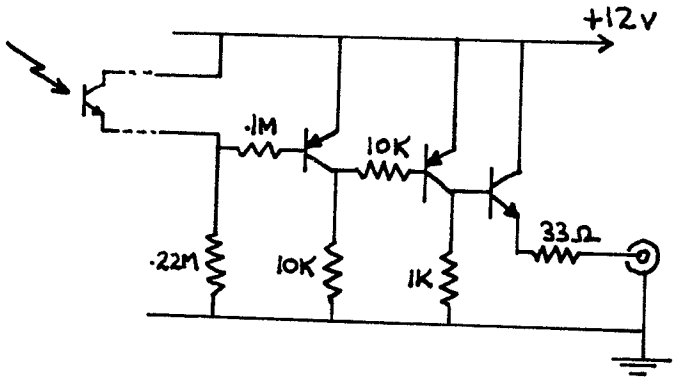

Fig. 3.9 Phototransistor amplifier circuit.

has a maximum value of 2.5μ seconds and so this does not affect the marker pulse in any way.

The pulse output from the phototransistor is shaped and fed to a 50 ohm output impedance driving amplifier for matching to the cables back to the control room.

(c) Square wave to Sine wave converter

In the design considerations of Chapter 2, a distortion of the cylindrical surface scanners was mentioned. The projected motion of the scanning wire onto a diameter is simple harmonic. Fig. 3.10 is a schematic of the situation. The displacement of the wire is given by:

$$X = R \cos(\omega t + \phi)$$

where

R = the radius of the scanning arm

ω = the angular frequency of the motor

ϕ = phase difference

for simplicity assume that at $t = 0$, $X = R$ then $\phi = 0$ and the velocity of the wire is given by:

$$\dot{X} = -R\omega \sin\omega t$$

Thus the projected velocity varies from 0 at each end of the diameter of the circle of revolution to a maximum $R\omega$ when the wire is at the centre of the beam tube. The oscilloscope trace moves across the screen at a constant rate and therefore the profile display is somewhat distorted. This problem is

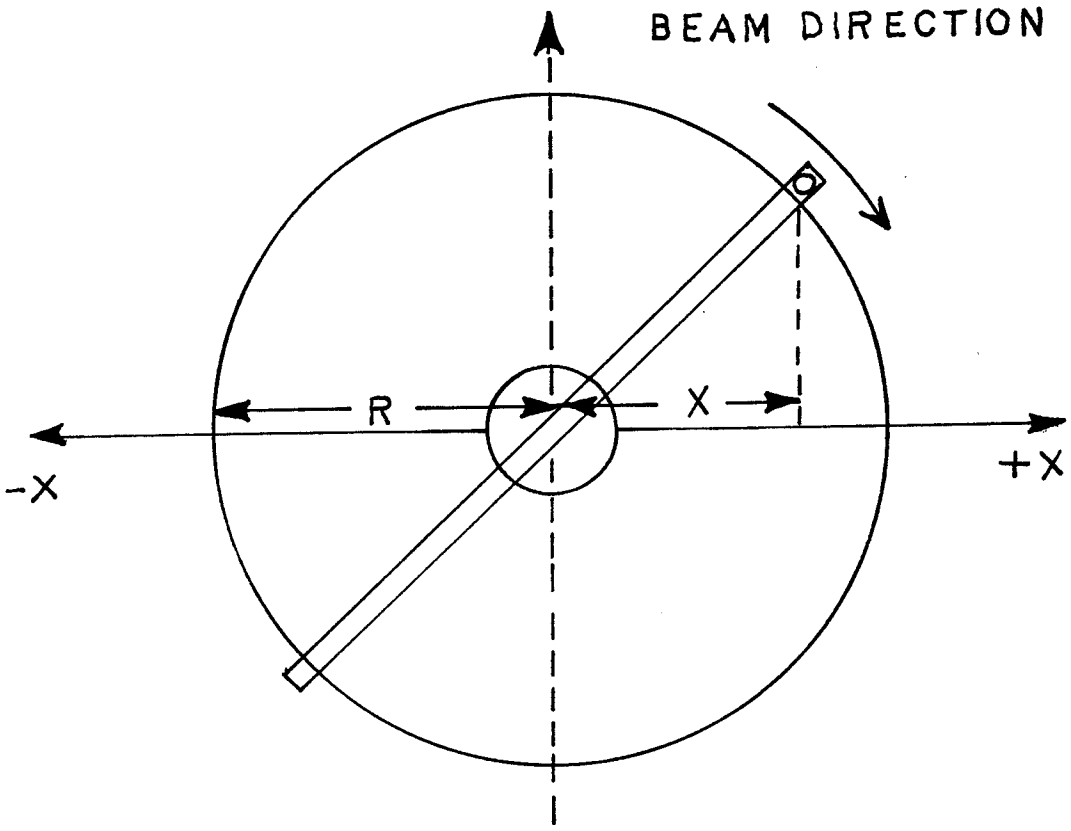

Fig. 3.10 Projected motion of the scanning wire.

overcome by providing a sinusoidal sweep for the oscilloscope, derived from the square wave output of the light encoder. Fig. 3.11 shows the conversion. Waveform I is the square wave output from the light encoder which is integrated by an operational amplifier integrator to give the triangular waveform II. The triangular waveform is filtered to give a sinusoidal waveform III. For a synchronous motor the filtering is accomplished very effectively by setting the gain of an active filter to its maximum at the frequency of rotation of the motor. However here we were not using a synchronous motor and effective filtering was performed by passing the triangular waveform through a diode circuit. The threshold of the circuit was set so that the "knee" part of the diode characteristic was used to operate on the triangle wave to give a very good approximation to a sinewave at the output. The resulting sinewave then forms the horizontal sweep of the oscilloscope, the scope is triggered from the leading edge of the square wave and blanked by the falling edge. The oscilloscope controls can then be adjusted so that the amplitude of the sinewave is proportional to $R\omega$. The profile then displayed is a true representation of the beam profile. The square wave to sine wave converter is shown in Fig. 3.12. The 10KΩ variable resistor sets the sinewave output so that its shape is symmetric around 0 volts. Operational amplifier #1 forms the integrating circuit and operational amplifier #2 has the diode arrangement in its feedback loop for filtering of the triangular waveform.

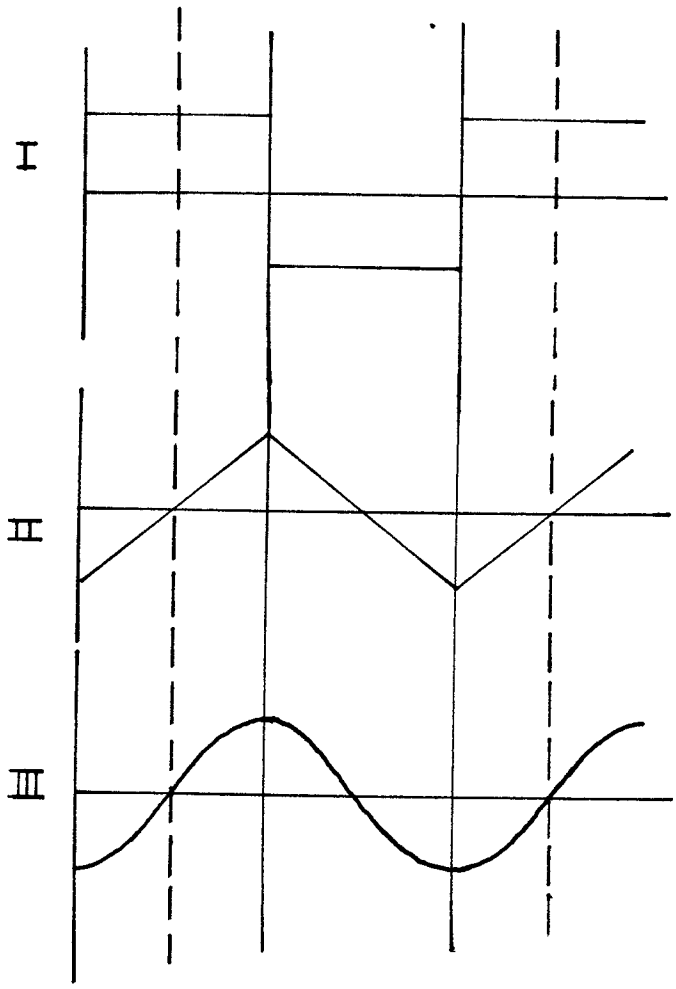

Fig. 3.11 Waveform conversion for a sinusoidal oscilloscope sweeping.

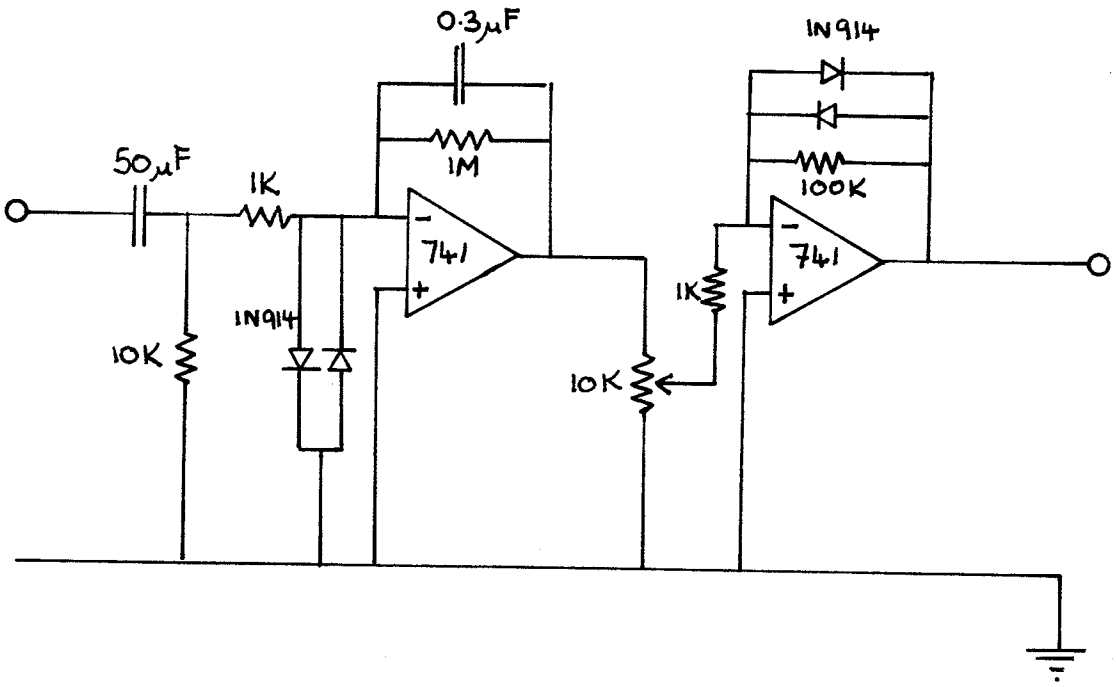

Fig. 3.12 Square to sine wave converter circuit diagram.

(d) Beam profile amplifier

The output from the wire pickup is fed to the beam profile amplifier shown in Fig. 3.13. An F.E.T. input RCA3130T operational amplifier was chosen for its high input impedance ($1.5 \times 10^{12}\Omega$) and low input current (5 pA). The gain of the amplifier is set by the parallel combination R_1 and C_1 and adjusted by VR_1. The zero adjust is performed by VR_2. The output of the operational amplifier is fed to a long tailed pair (Q_1 and Q_2) arrangement followed by a driver amplifier to drive a 50Ω cable back to the control room. The beam profile amplifier was mounted in a small aluminium box and attached to the side of the scanner to keep the input lead as short as possible which would reduce pickup from the R. F. supply of the cyclotron.

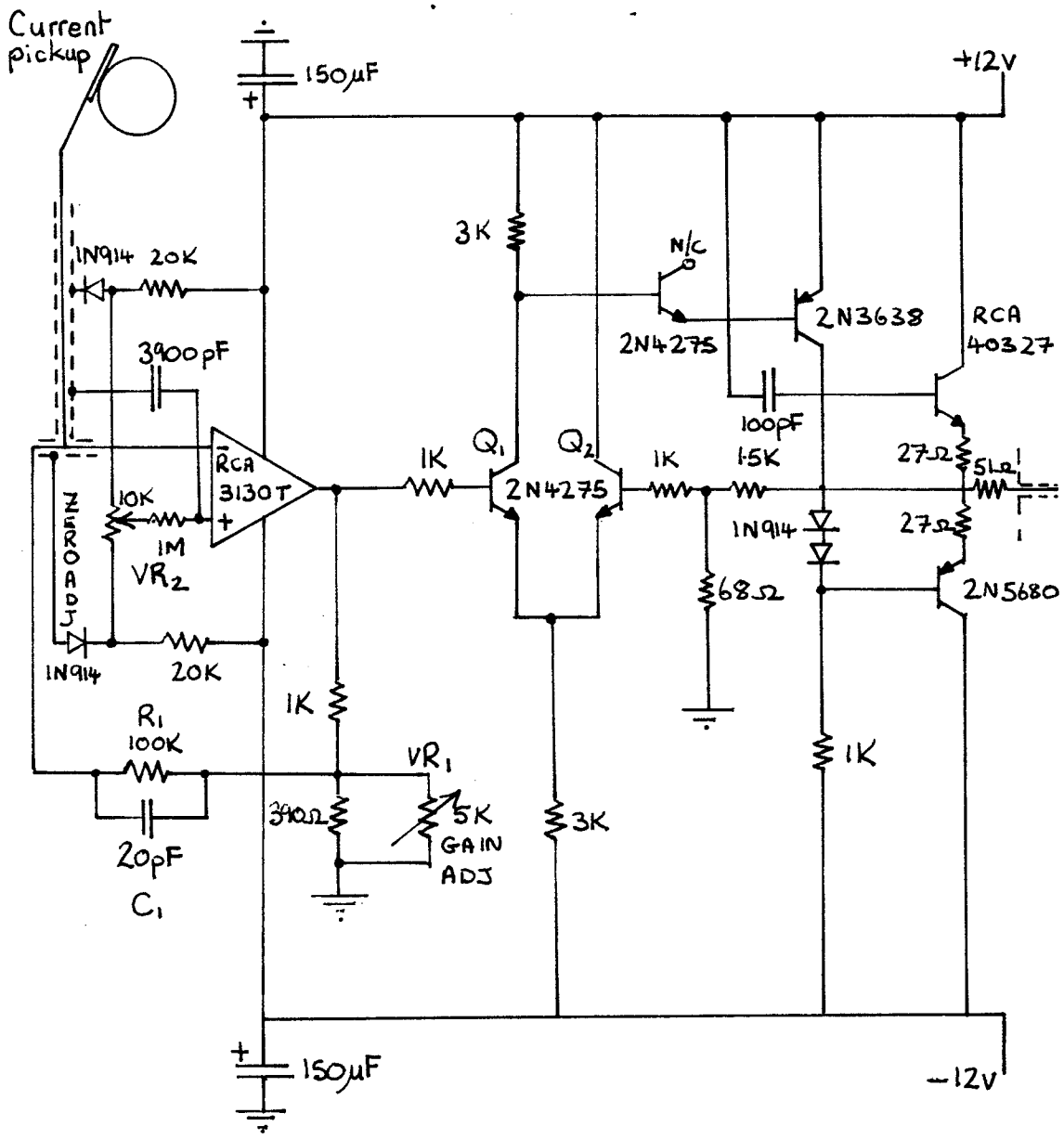

Fig. 3.13 Beam profile amplifier circuit diagram.

III. NOISE SOURCES AND THEIR REMOVAL

In this section the unwanted part of the signal from the beam scanner is discussed. I have called all these signals "noise" and a discussion of their sources and removal follows.

(a) Thermal noise Shot noise and 1/f noise

Fluctuations around the most probable values of the energy of electrons in a conductor are small but give rise to potentials which manifest themselves as noise called Thermal or Johnson noise.

The mean square noise voltage is given by:

$$V_n^2 = 4KTR(f_h - f_l)$$

where R = resistance

T = temperature

K = Boltzman's constant

$(f_h - f_l)$ = the band-width over which the noise is measured

This type of noise accounts mainly for that produced in resistors.

Shot or Shottky noise is produced by the fluctuations in the number of discrete charged particles flowing in a semi-conductor for example from emitter to collector in a transistor. The time average of these fluctuations is the current flowing in the device.

The mean square value of noise current is given by:

$$I_n^2 = 2qI_{d.c}(f_h - f_l)$$

The noise voltage produced across a resistor will therefore be:

$$V_n = I_n R_L$$

where:

q = electronic charge

$I_{d.c}$ = d.c current

$(f_h - f_l)$ = bandwidth over which the noise is measured

R_L = load resistor

1/f noise - the mechanism of this noise source is not fully understood, it varies as 1/f where f is the frequency of the signal and so predominates at low frequencies.

(b) Transistor noise

In n-p-n and p-n-p type transistors random motion of electrons crossing emitter and collector junctions and random combinations of electrons and holes in the base give rise to transistor noise. In field effect transistors (which have low noise characteristics) the main sources of noise are thermal noise of the resistance of the conducting channel, shot noise caused by the gate leakage current and 1/f noise caused by surface effects.

(c) Discussion

The most important contribution to the noise at the output

of the beam profile amplifier is that which occurs at its input since this is multiplied by the full gain of the amplifier along with the beam current signal. Thus the most important noise that occurs is that in the F.E.T. input section of the operational amplifier. Fortunately, field effect transistors have low noise figures and with the gain control set at a typical value all the noise sources discussed above would result in 0.1 volt "white" noise at the output (i.e. approximately the same noise power per unit bandwidth).

There are various ways of reducing these noise sources, the most obvious way is to reduce $(f_h - f_l)$ that is the bandwidth of the amplifier, this is already reduced somewhat in the beam profile amplifier described above since the gain is set high. The bandwidth can be further reduced by using a tuned circuit amplifier input. The mean square noise voltage can be reduced by running the amplifier at a low temperature. However, other noise sources were present at the output of the beam profile amplifier, these consisted of 60Hz, 120Hz and radio frequency pickup signals of various amplitudes superimposed onto the noise sources described above. These signals were originally many times the magnitude of the Thermal noise etc. Since they were difficult to isolate individually, their reduction to a minimum formed a major part of the development of the first scanner eventually leading to a second version described in the next chapter. These "scanner generated" noise sources and their solution are described below.

(d) Pickup noise

Many types of materials used in the current pickup were tried and as described above a copper strip with a phosphor-bronze "dot" at the end proved to be the best. However, the pickup would eventually pit the surface of the collar on the rotating arm and the noise level at the output would then become steadily worse. The extra drag imposed on the motor shaft would also cause a fluctuation in the motor speed which manifested itself as a stretching and shortening of the square wave output. Having to vent the vacuum system for regular cleaning and polishing of the pickup would be a real problem for maintainance technicians in the event of several scanners being installed in the accelerator structure.

The noise level generated by the rotating pickup was approximately 2 volts p-p 60Hz (depending on the gain setting) when the contact was badly worn.

In the first tests of the scanner using actual beam, we hoped for a high enough signal to noise ratio that the brush noise would only be a problem when the brushes needed to be cleaned or changed. However in these tests no clear profile could be seen.

(e) A cylindrical drum pickup

It was decided at this stage to abandon the brush type pickup. Secondary electrons escaping from the wire would be collected. A cylindrical pickup, insulated from the beam

line and scanner housing would collect the electrons forming a contactless pickup which would not have the brush noise generated by the first type.

The pickup was made in such a way that it would provide the maximum surface area to collect the electrons, while being the easiest to mount in the beam line. A cylindrical can was made from aluminium with two holes much larger than the beam diameter machined out.

The scanner was mounted on the underneath of a standard four inch beam cube and the can was lowered in from the top. Teflon rings insulated the can from the beam line and scanner housing. Other ports on the cube were closed off with standard aluminium blanking plates to substantially reduce the 60Hz pickup by the can.

The can would detect any vibrations of the cube or the beam line structure and would send these as a signal into the beam profile amplifier. This microphonic noise source resulted in a 60Hz sinewave of several volts peak to peak at the control room output. The teflon ring which spaced the can away from the beam line was removed. The can was machined accurately enough that it would stand away from the (grounded) beam line without any spacer. This ring was coupling the vibrations of the motor to the can and its removal reduced the noise level considerably. The length of the rotating arm was shortened to 6.3 cm, this would still give a larger scanning radius than any beam size encountered and this reduced further the vibrational

pickup since any effect of the arm being unbalanced would be less pronounced.

The light encoder on the lower shaft of the motor was made in the form of a cut out aluminium drum. The cut out resulted in more vibration of the motor since the load on its shaft was unbalanced. This was solved by machining the encoder from plexiglass and painting on the shapes of the cut out required to block the light.

(f) Summary

The multiple sources of noise in the signal from the beam scanner were reduced to a minimum by balancing loads on the motor shaft.

The original signal noise levels from the cylindrical pickup were approximately 10 volts peak to peak, these were reduced to 0.3 volts peak to peak superimposed on 0.1 volt white noise.

The first version of the scanner was thus in its working form. Its inherent disadvantages and a second version of the scanner are described in Chapter 4.

CHAPTER 4

A SECOND GENERATION BEAM SCANNER

INTRODUCTION

Working on the prototype beam scanner has shown its disadvantages. It was an awkward and time consuming exercise to replace the bulb in the light encoder or to change a faulty 'O' ring vacuum seal on the scanner housing. Both would involve venting the vacuum system and removing the base plate of the scanner. Indeed before an 'O' ring could be replaced all the soldered base plate connections had to be removed and later re-soldered. Furthermore, the plexiglass light encoder would tend to slip and re-tightening involved dismantling the scanner followed by re-alignment with a stroboscope.

With these disadvantages in mind a second generation scanner was designed. In this version the scanner housing contains only the motor. The position encoding of the scanning wire and the scanning wire itself are mounted around the shaft of a single ended motor.

The whole scanner weighs much less than the prototype and the vibrational pickup is much less. Mechanical and electrical details of this scanner are given below.

I. MECHANICAL DETAILS

The scanner housing was made of brass so that the vacuum feedthrough for power etc. could be welded to the side of the housing. The base plate can then be removed if necessary without interrupting any of the connections. A tape player Matshoshita 4ZSC23UO4P synchronous drive motor was used in this version, a small motor $1^{7}/_{8}$ inches in diamter and 2 inches long consuming 10 watts of power. The motor and the starting capacitor are the only components inside the scanner housing.

The length of the rotating arms was kept at 6.3 cm but the other dimensions of the arm were made much smaller. The arms was made from 1/8 inch diamter brass rod, the collar which fits on the motor shaft was correspondingly smaller. The scanner is shown in Fig. 4.1.

Encoding of the wire position is accomplished by two Texas instruments TIL146 optoelectronic encoders, these can also be seen on the scanner in Fig. 4.1 mounted on opposite ends of a diameter perpendicular to the beam direction. When a short wire 0.5 cm long attached to the rotating arm on the scanner passes through a space in the encoder a pulse is generated which when processed will give the square wave position output of the scanner. The encoder is described fully in the electronic details. The cylindrical pickup from the prototype scanner remains and the complete scanner is shown mounted in a standard beam cube in Fig. 4.2

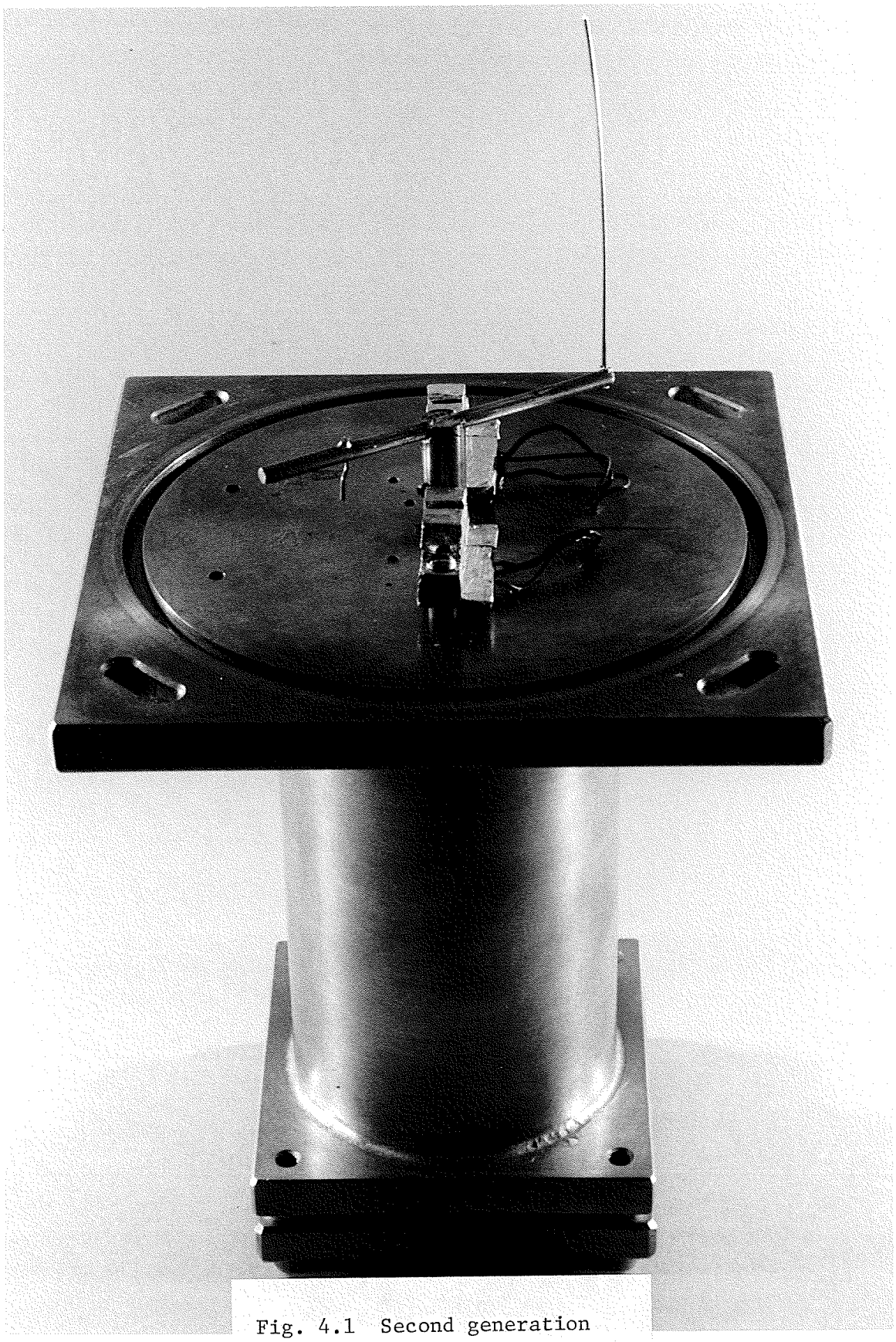

Fig. 4.1 Second generation beam scanner.

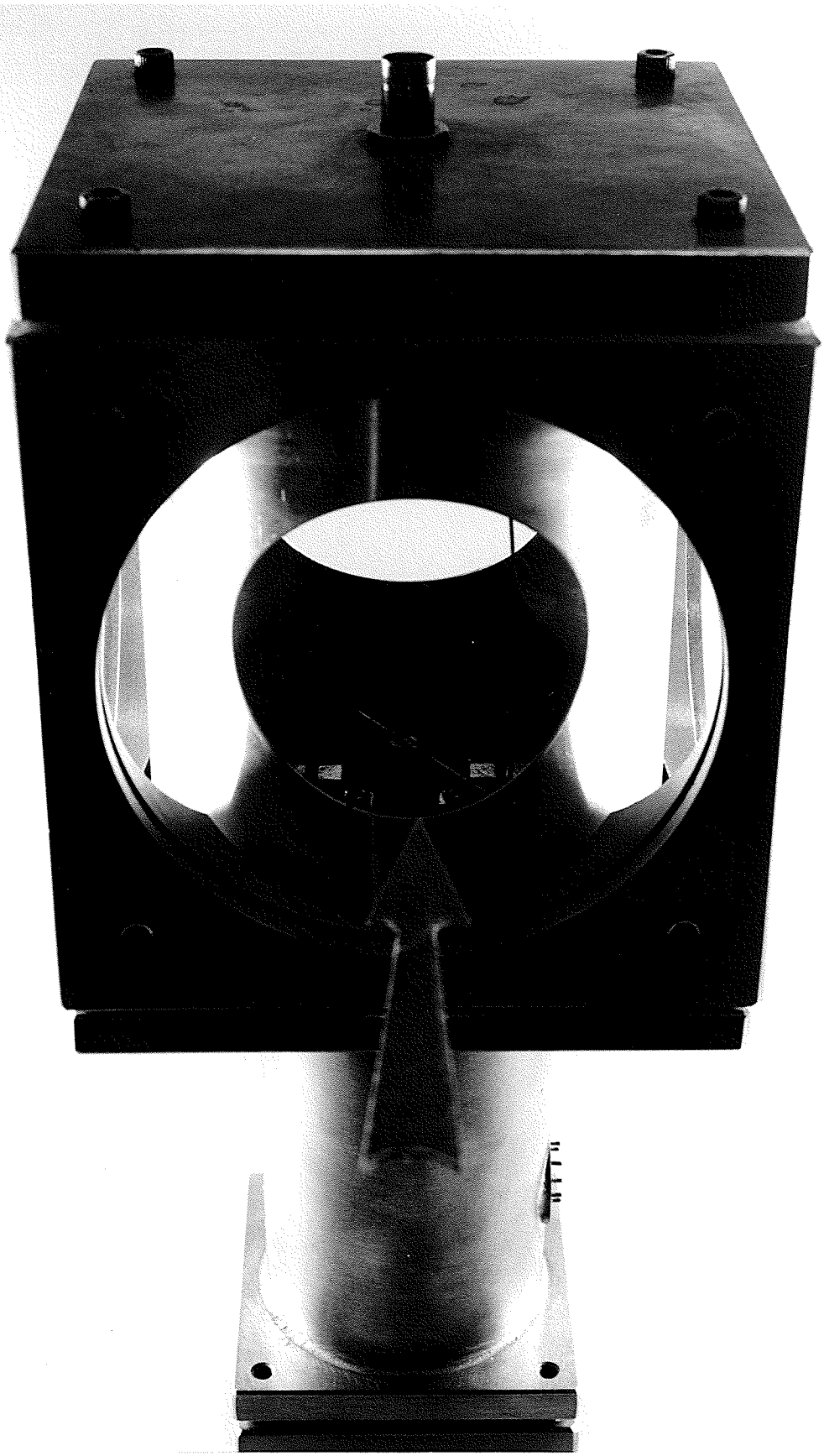

Fig. 4.2 Scanner and cylindrical pickup mounted in a standard beam cube.

II. ALIGNMENT

The wire position encoding devices are mounted at each end of a diameter perpendicular to the beam direction. By simply attaching the scanner to the beam cube, the scanner is aligned quite accurately. Only the accuracy with which the encoders are installed creates a misalignment, in the event of this the holes on the scanner housing have been elongated and the pulse output from each encoder can be used to trigger a stroboscope to show that the wire position is at the end of a diameter. No pulse output to show beam tube centre is incorporated into the electronics for the scanner since the beam tube centre corresponds to the mid-point of the square wave.

III. ELECTRONIC DETAILS

(a) Light Encoder

Each encoder assembly consists of a gallium arsenide infra-red emitting diode and an n-p-n silicon Darlington transistor mounted in a housing made from 40% glass filled polyphenylene sulphide plastic.

When the light output from diode to transistor is interrupted by the wire a pulse is produced. This pulse is amplified to drive a set-reset type flipflop. As the wire begins the scanning cycle a pulse from one of the encoders sets the flipflop output to +5 volts d.c. As the wire completes a scan another pulse resets the flipflop to 0 volts. The circuit is shown in Fig. 4.3. In this way, a square wave output is obtained with the same frequency as the angular frequency of the motor. The electronics for converting the square wave to a sine wave are the same as for the prototype scanner.

(b) Beam profile amplifier

It was found when using the prototype scanner that the d.c. level of the output would shift with beam optics settings. To change the d.c. level control or gain control meant switching off the beam to enter the accelerating vault to change the potentiometer settings. For the second version a remote control facility was incorporated for the d.c. level and gain

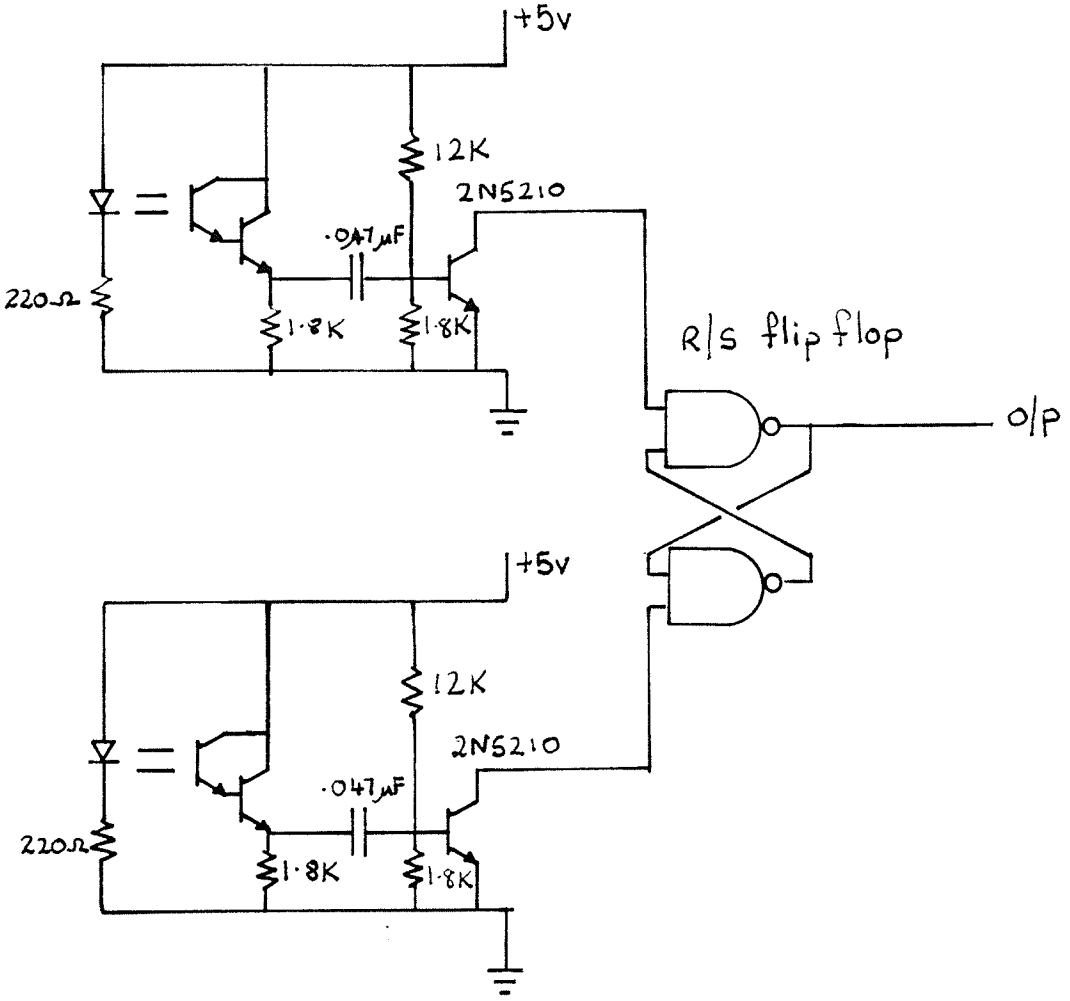

Fig. 4.3 Square wave generating circuit for the second generation scanner.

controls. The potentiometers were removed from the beam profile amplifier box and rack mounted together with the beam scanner power supply unit. The leads were kept as short as possible to reduce any kind of pickup. A Hankscraft company 3440-30R-3V d.c. motor was connected to the shaft of each potentiometer. These motors were internally geared to 30r.p.m. and when actuated from the control room provided remote gain and d.c. level controls. The rest of the beam profile amplifier was unchanged. The complete beam scanning arrangement showing scanner, pickup, power supplies and remote gain control unit is shown in Fig. 4.4.

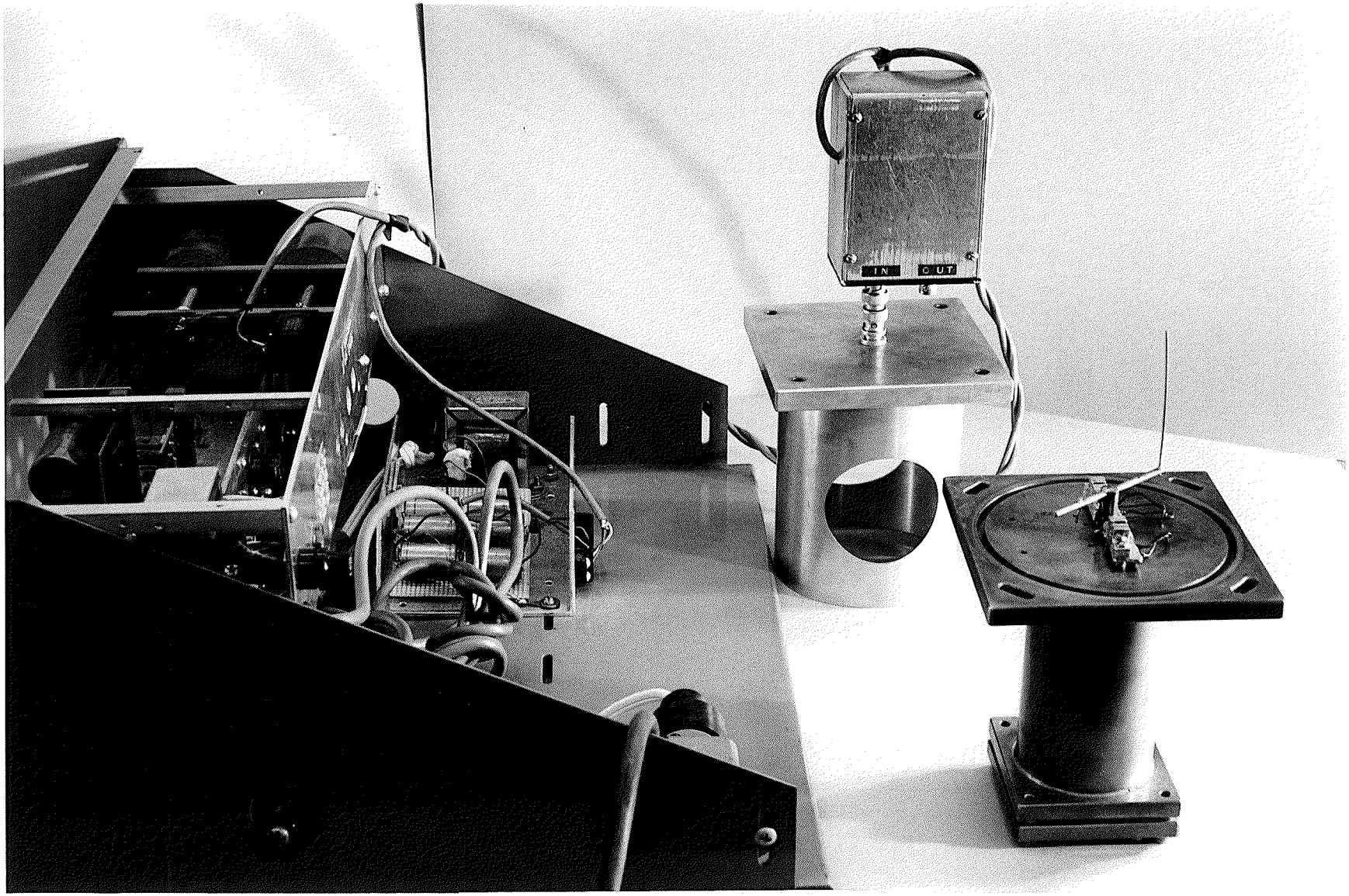

Fig. 4.4 The complete scanning arrangement showing scanner, pickup and electronics.

IV. NOISE LEVELS

In this scanner the noise consisted of the 0.1 volt white noise from the beam profile amplifier and this has 0.15 p-p 60 Hz vibrational pickup superimposed on it when the scanner is actuated.

Multiple groundings on the lines back to the control room also caused pickup problems. Eventually, a single 50Ω co-axial cable was run from the accelerating vault to the control room for the beam profile output. This cable was grounded to the beam line only.

The next chapter shows typical results obtained with this scanner.

CHAPTER 5

BEAM PROFILES

INTRODUCTION

At this point in the development of the beam scanner a unit exists with an output noise level of 0.15 volt 60Hz vibrational pickup superimposed on 0.1 volt noise from the amplifier.

In this chapter, beam profiles are shown at two points in the accelerator structure. (I) In the 0° beam line and (II) in the polarized ion source where it was found that the scanner would also give an intensity profile of a beam of neutral particles.

I. THE ZERO DEGREE (0°) BEAM LINE

This beam line is the exit beam tube of the accelerator where beams of up to 5μ Amperes of 50 MeV protons can be produced.

Fig. 5.1 shows the beam scanner outputs in the absence of a beam. The 5 volt square wave allows beam displacement to be read from the oscilloscope screen, the middle of the square wave corresponds to the centre of the beam tube. The output noise from the beam profile amplifier is shown as the lower trace.

Fig. 5.2 shows a typical profile. A 675 nano-Ampere beam of 28 MeV protons was focussed to 8 mm width at the position of the scanner. The profile height is 6.5 volts and with the 0.2 volt p-p noise output gives a signal to noise ratio of 32.5 times or 30 dB. All the profiles shown here are 'X' direction cross-sectional intensity profiles.

In Fig. 5.3 the beam was defocussed at the position of the scanner to 2.6 cm wide. Since the scanner is sensitive to current density i.e. 675 nA over 2.6 cm the profile height decreases somewhat. The signal to noise ratio here is 20 dB.

Fig. 5.4 and 5.5 investigate the limit of resolution of the scanner for low beam currents. In Fig. 5.4 the profile is still clearly visible (signal to noise ratio 6 dB) for a beam current of 32 nA focussed to 5 mm. The limit is shown in Fig. 5.5 where the beam width is more difficult to measure but is approximately 3 mm for a beam current of 18 nA. Thus

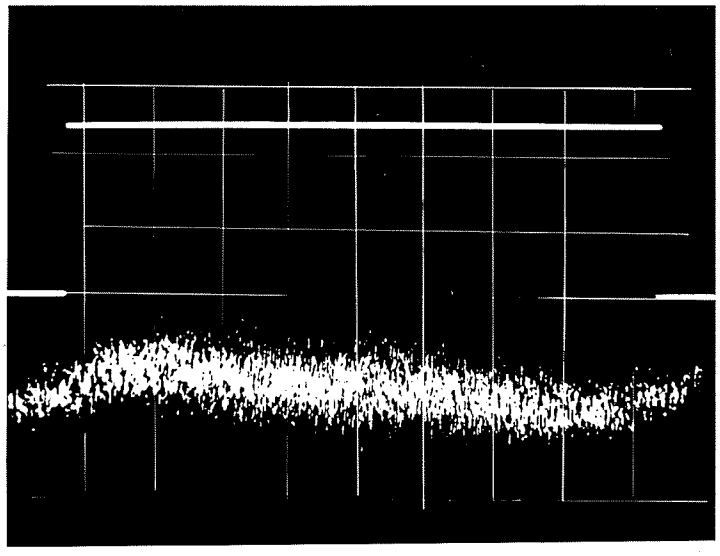

Fig. 5.1 Square wave output and beam profile amplifier output in the absence of beam.

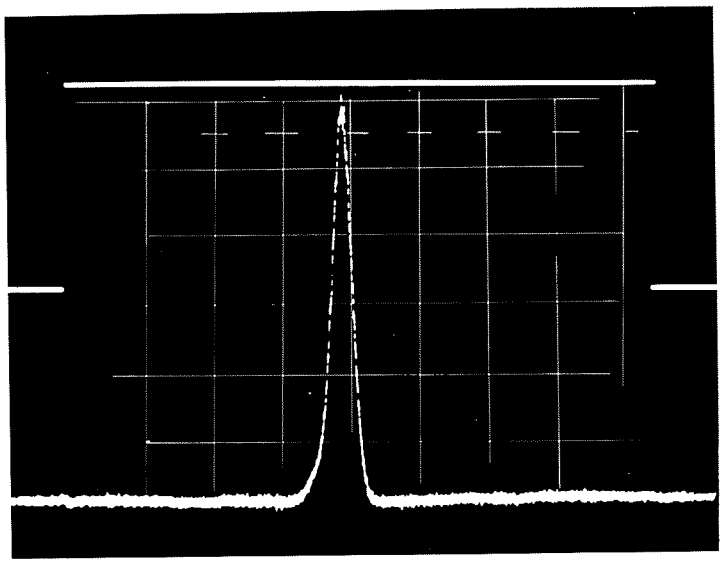

Fig. 5.2 Beam profile of a focused beam of protons.

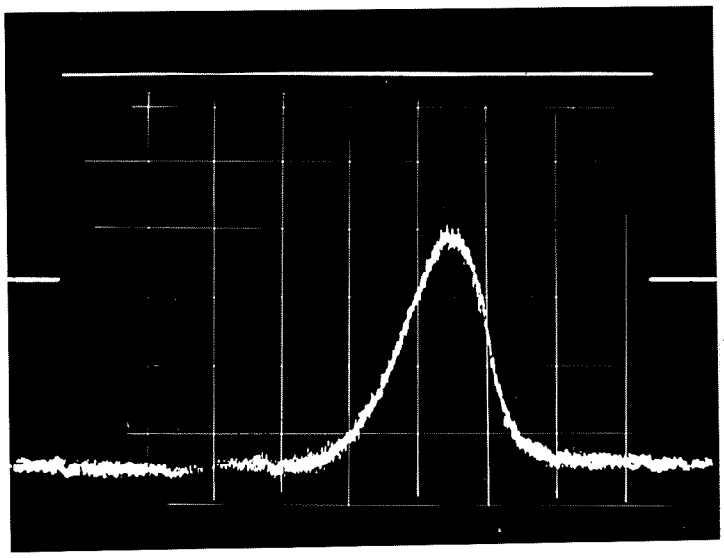

Fig. 5.3 A beam defocussed at the position of the scanner.

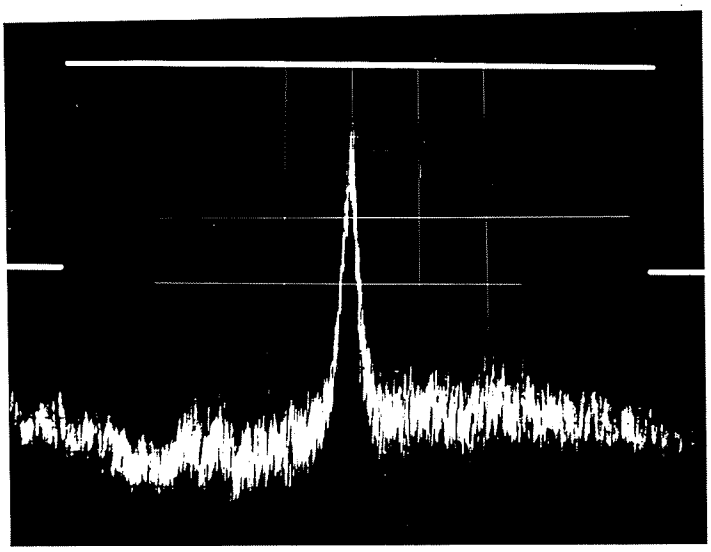

Fig. 5.4 Beam profile for low beam current (32nA)

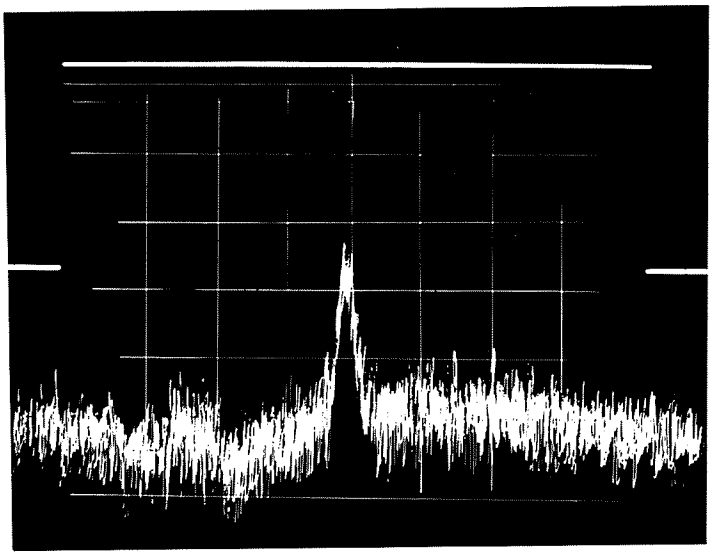

Fig. 5.5 The limit of resolution of the scanner. Beam current 18 nA

18 nano-Amperes is the limit of resolution of the scanner at this time.

II. POLARIZED ION SOURCE

The beam scanner was used in conjunction with the emittance measuring device described in the next chapter in the Summer of 1980 for some preliminary measurements of the emittance of the beam from the ceasium cell in the polarized ion source shown in schematic form in Fig. 5.6. The Argon channel was replaced by a drift space followed by the scanner.

At these low energies around 1100 eV the secondary electron emission is much higher and beam currents are generally much higher in the ion source. In consequence no beam profile amplifier was necessary and the cylindrical pickup could be fed directly to an oscilloscope.

The most surprising and interesting discovery was that the scanner would also produce an intensity profile for the beam of neutral particles. Fig. 5.7 shows an intensity profile of a 4 mm wide beam of 1200 eV neutral deuterium atoms. The charged components of the beam were swept out of the way by a magnet. In Fig. 5.8 two charged components of the beam are also shown.

After approximate measurements of the emittances in the ion source hall the emittance of the cyclotron was to be measured, and this is described in the next chapter.

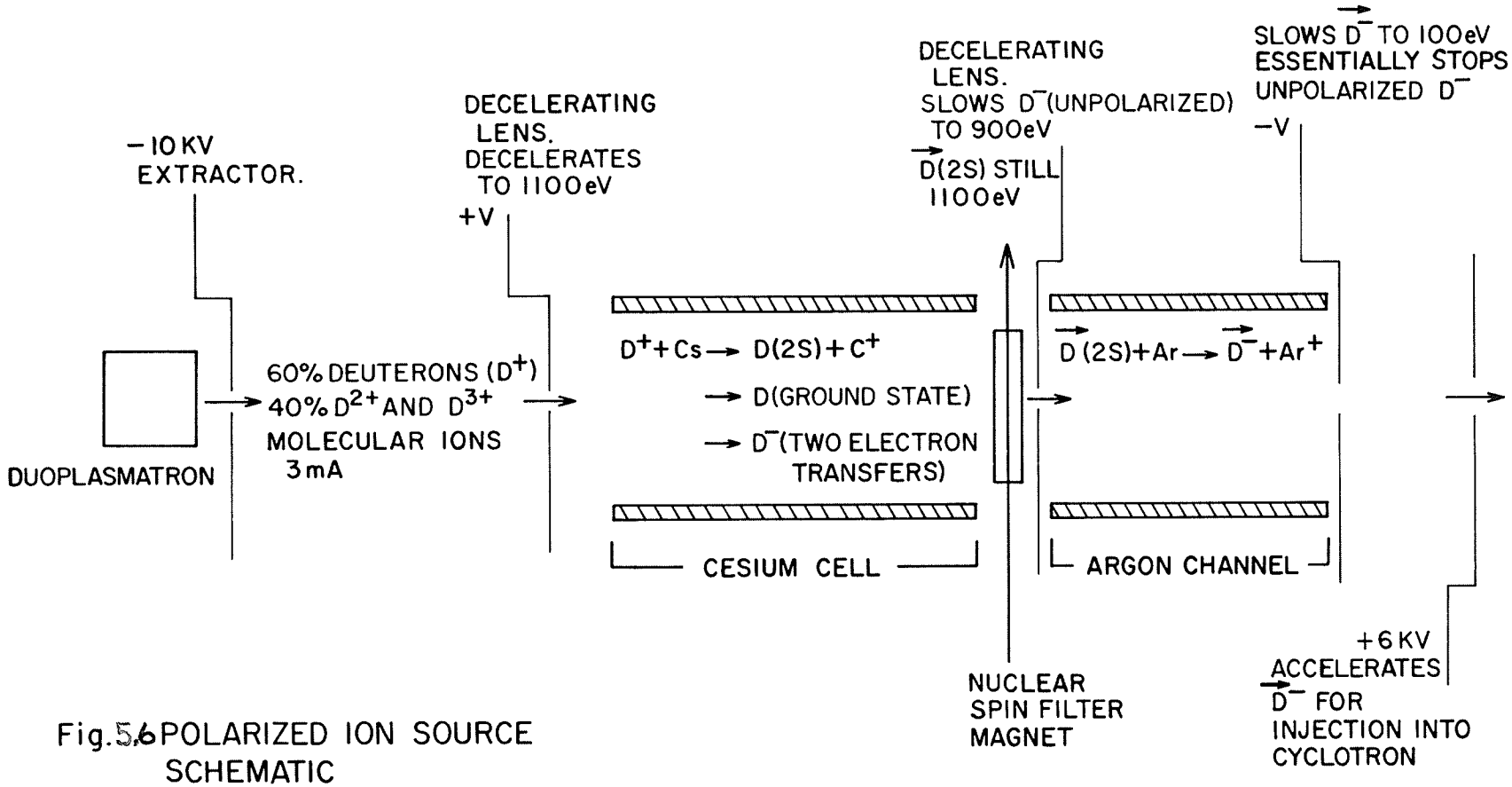

Fig. 5.6 POLARIZED ION SOURCE SCHEMATIC

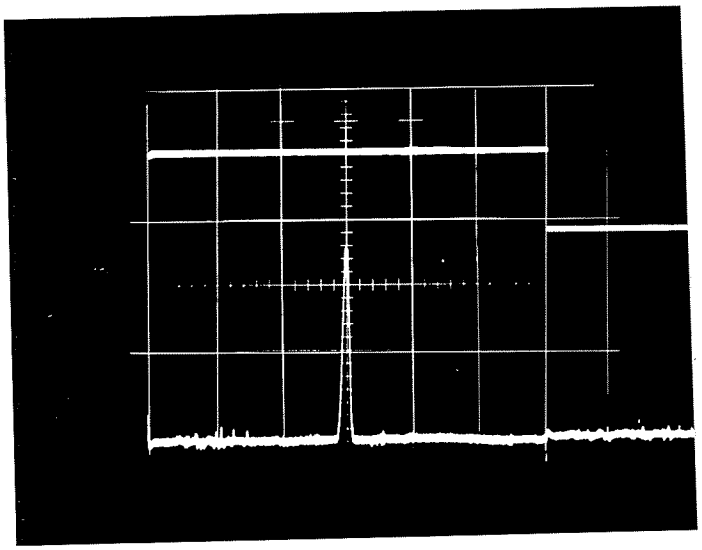

Fig.5.7 A beam profile of a beam of neutral deuterium particles.

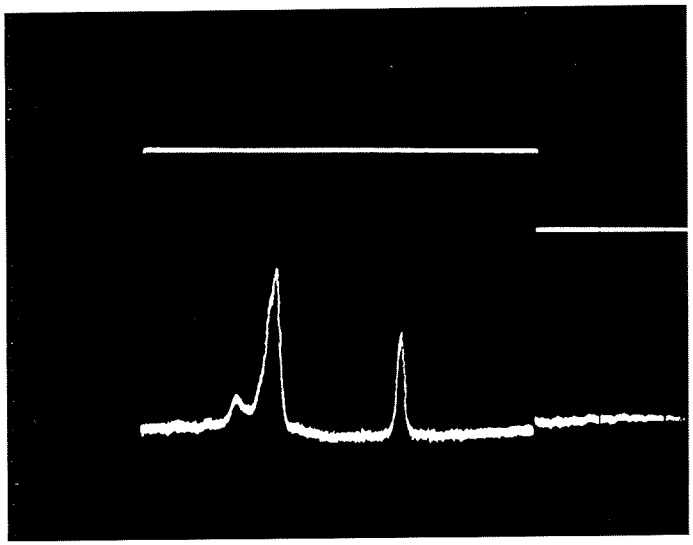

Fig. 5.8 Beam profile showing neutral beam and two charged components.

CHAPTER 6

EMITTANCE OF THE CYCLOTRON BEAM AND ITS MEASUREMENT

INTRODUCTION

When transporting the charged particle beam from the ion source to the accelerator or from the accelerator to the experimental area one would like to keep as much of the beam current as possible.

The factor which governs how much beam can be transmitted to the beam lines from the accelerator for example, is the emittance of the cyclotron beam.

The emittance describes the divergence of the beam at different points across its cross section. For complete transmission the beam line has to be matched to the emittance of the cyclotron in much the same way as the impedances of transmission lines have to be matched.[17]

Sophisticated computer programs which take into account focusing elements, drift spaces etc. can predict beam spot size and divergence on target once the emittance is known. The concept of emittance and the hardware for the measurement of emittance are discussed in this chapter.

I. CONCEPT OF EMITTANCE

If one knows the position co-ordinates (X_i, Y_i, Z_i) and momentum co-ordinates (P_x, P_y, P_z) of all the particles in a beam then it can be specified completely as a 6 dimensional phase space hypervolume. The fundamental conservation law of Liouville states that under the action of conservative forces (e.g. produced by macroscopic electric and magnetic fields) the motion of such a collection of particles is such that the local density of the points in phase space remains constant.[18]

If the three components of the motion are mutually independent in real space (assuming no space charge effects) then in phase space the motion is confined to three planes (X, P_x), (Y, P_y), (Z, P_z). In this case Liouville's theorem simplifies to saying that the area of the shapes in these planes remains constant. The angular divergence of a particle in the beam is equal to the ratio of the transverse and axial momenta, since the latter is constant we can replace P_x (transverse momentum) by angular divergence $X' = dx/dz$ and the co-ordinates of the two dimensional phase space become x and x' which are both directly observable. Thus the area of the phase space contour in the x,x' plane is a constant, this area is known as the emittance area of the beam with units of millimeter milliradian (mm - mrad). The complimentary concept

to emittance is acceptance and refers to a piece of equipment rather than a beam. Acceptance is the phase space area containing all the points whose co-ordinates represent particles that would be accepted into the aperture.

For matching of a beam to an aperture we must match the emittance in both area and orientation to the co-ordinate axes, as shown in Fig. 6.1. Space charge effects become weaker as beam energy increases and need not be taken into account for the emittance of accelerators. However they do need to be taken into account for the emittance of ion sources.

What shapes of emittance contour does one expect to find? Under the influence of a restoring force proportional to the instantaneous displacement x of a particle from the beam axis, the particle will exert simple harmonic motion given by:

$$\frac{d^2x}{dz^2} = -\left[\frac{2n}{\lambda}\right]^2 x$$

where: λ - is a constant depending on the restoring force

Z - axial direction

x - transverse direction

The solution is a sinewave of amplitude 'a' and phase ϕ given by:

$$x = a\ \mathrm{Sin}\left(\frac{2nz}{\lambda} + \phi\right)$$

and

$$\frac{dx}{dz} = \left(\frac{2n}{\lambda}\right) a\ \mathrm{Cos}\left(\frac{2nz}{\lambda} + \phi\right)$$

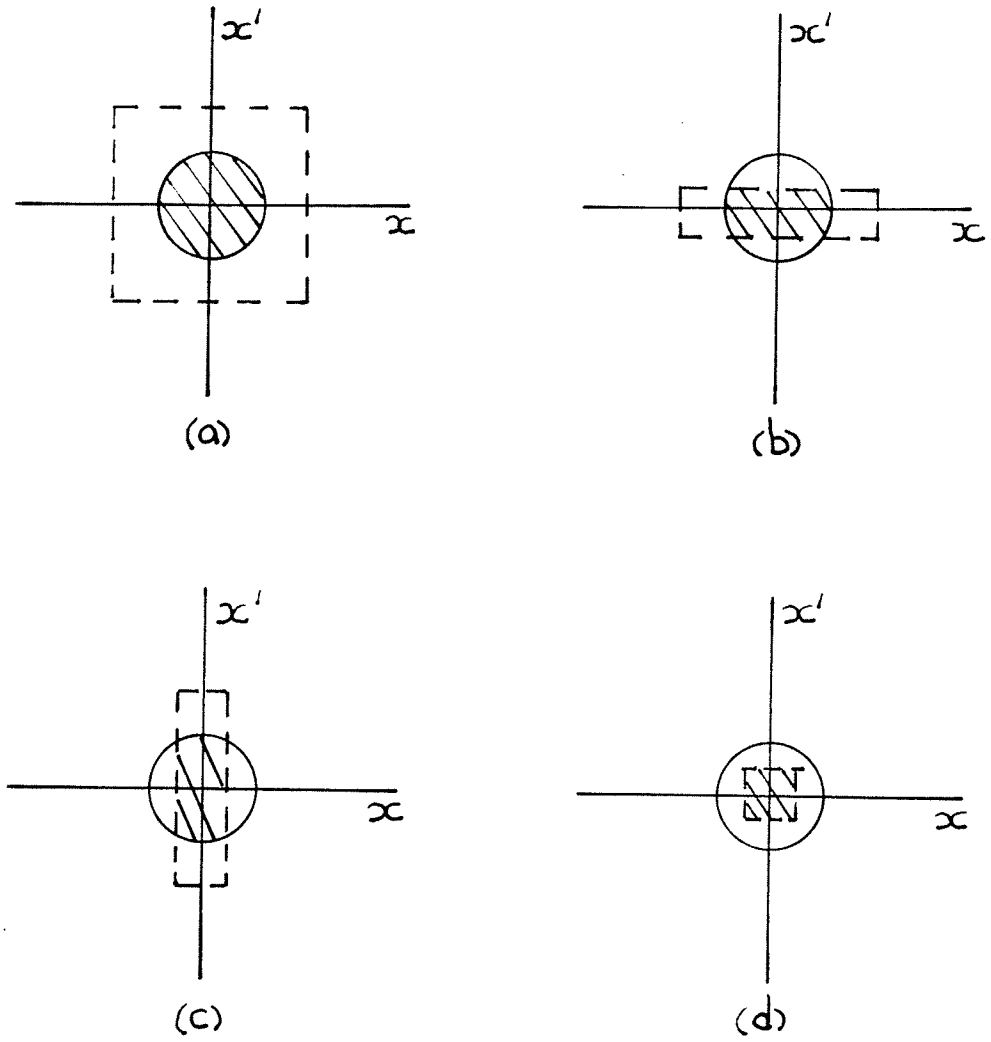

Fig. 6.1 The acceptance of hypothetical device is represented by the circles and the emittance of the input beam by the dashed rectangles. The transmitted beam is shaded. In (a) the beam emittance is too big for complete transmission whatever its shape. In (b), (c) and (d) the emittances are all equal and less than the acceptance. Only in (d), where the beam is correctly shaped, is there complete transmission.

Eliminating $(\frac{2\pi z}{\lambda} + \phi)$ gives:

$$\frac{x^2}{a^2} + \frac{x'^2}{(\frac{2\pi a}{\lambda})^2} = 1$$

the equation of an ellipse. Thus the plot of displacement from beam axis versus divergence should ideally be an ellipse, points filling the ellipse represent particles with a different values of amplitude 'a'. After the beam leaves the accelerator the ellipse becomes tilted if the beam flows in a drift space. If there are momentum defining slits at the exit of the accelerator then the emittance shape will have straight line boundaries.

Non-linear forces acting on an elliptical emittance shape would distort the contour. However it is still convenient to describe the beam in terms of an ellipse and so a larger ellipse is drawn around the distorted contour. In this way the emittance is effectively increased by the action of non-linear forces.[19] The increase is shown diagramatically in Fig. 6.2.

The next section discusses the hardware for and the measurement of the emittance of the beam from the university cyclotron.

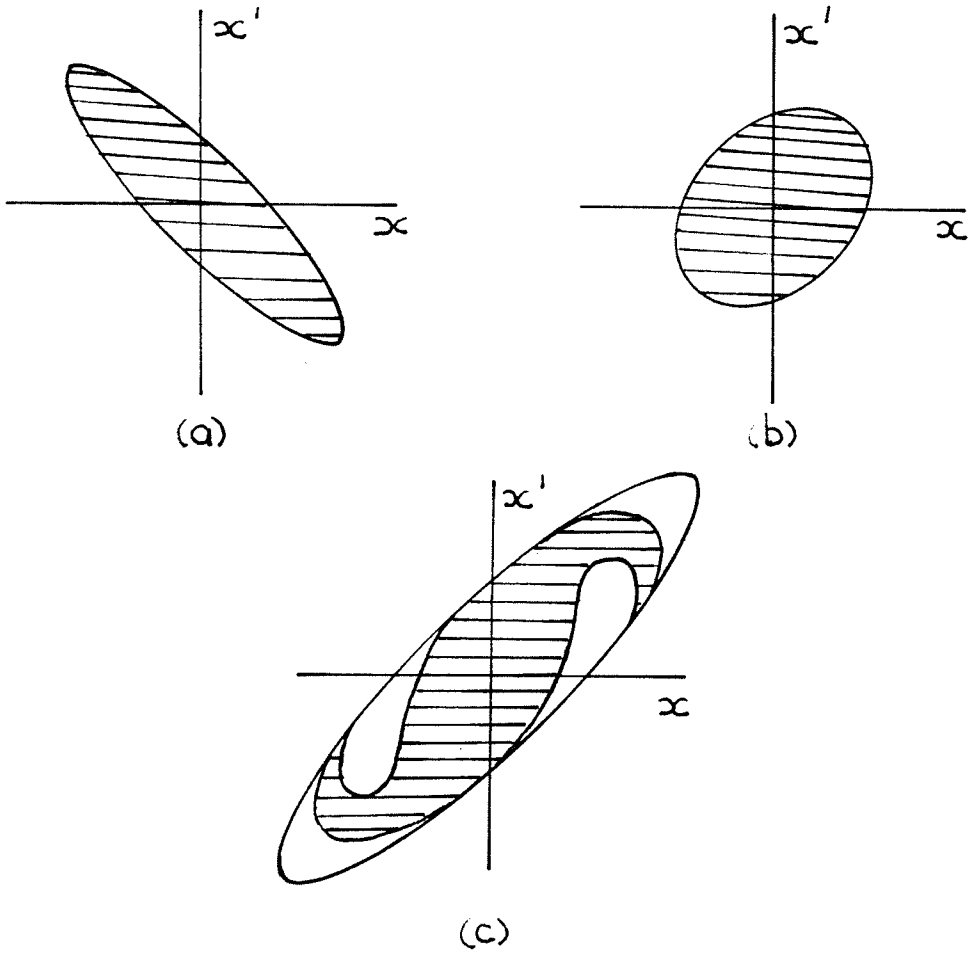

Fig. 6.2 The elliptical contour in (a) transforms to the ellipse in (b) under the action of linear forces and to the distorted countour in (c) under non-linear forces. All three shaded areas are equal the ellipse enclosing C defines the effective emittance of the beam and is greater than (a).

II. EMITTANCE MEASUREMENT

To measure the emittance of the cyclotron beam we need to make a plot of the displacement of a small filament of the beam from the beam tube centre versus the range of angular divergences for that filament.

Fig. 6.3 shows the schematic measurement. The displacement of the filament of beam current from beam tube centre is x. The particular filament chosen by the slit arrangement then passes through a drift space 'd' where a beam scanner detects it. The beam scanner output gives positions X_1 and X_2 and from this data the range of angular divergences θ_1 to θ_2 for that filament can be calculated from:

$$\theta_1 = \tan^{-1}\frac{(X_1-X)}{d}$$

$$\theta_2 = \tan^{-1}\frac{(X_2-X)}{d}$$

The resultant plot for all filaments will give the emittance shape. To isolate a particular filament of beam a moveable 1.0 mm wide slit was placed in front of the accelerator opening to the beam line. The slit consists of a 4 mm thick copper face 9 mm x 33 mm set in a 16 mm thick carbon block 9 cm x 9 cm. The slit is positioned by a 72 r.p.m. reversible stepping motor. The motor drives a threaded shaft, a tapped brass block fits on the shaft and is fixed to a steel rod which drives the slit through a vacuum seal. The wiper of a precision linear potentio-

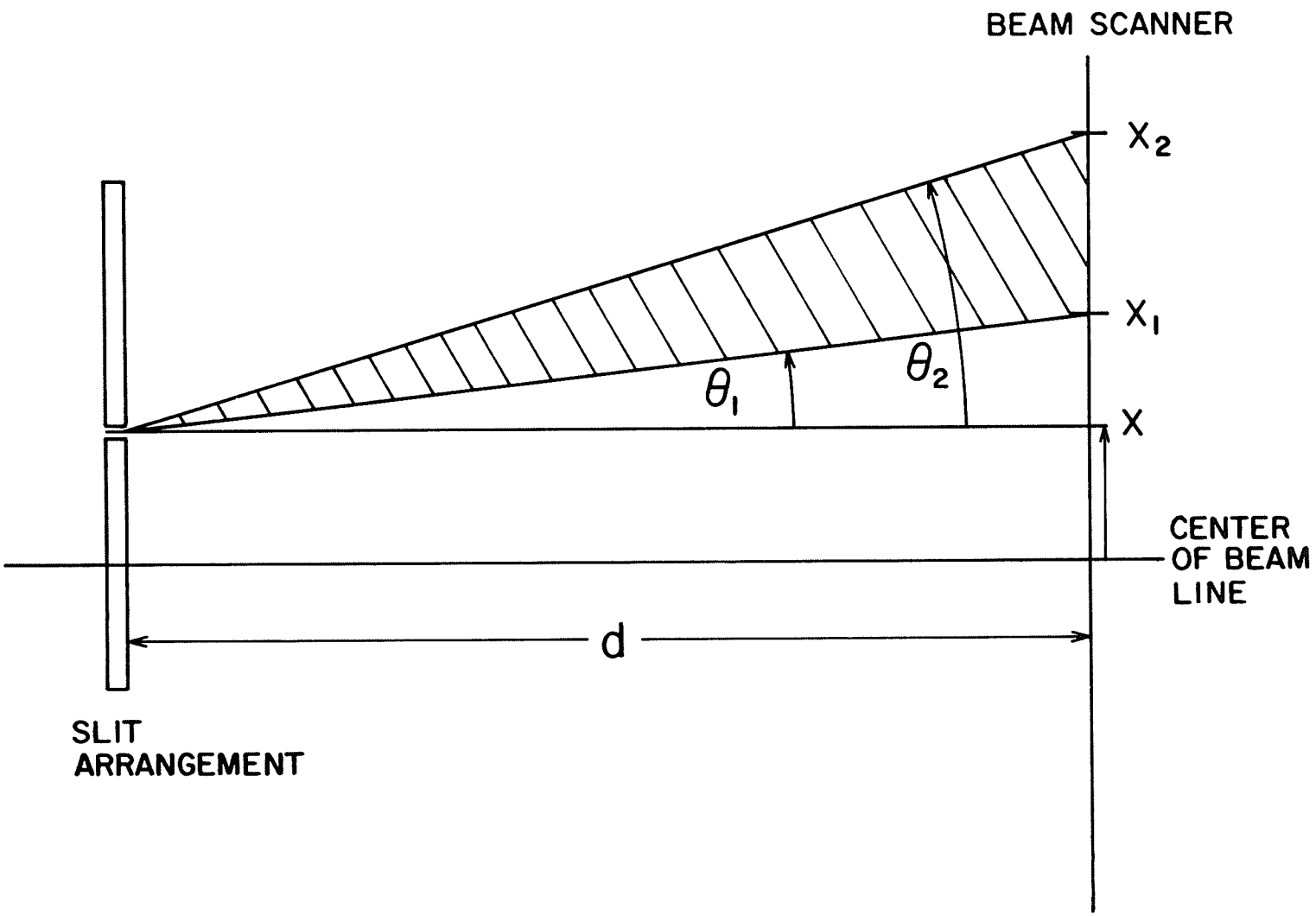
BEAM SCANNER
X_2
X_1
X
θ_1
θ_2
CENTER
OF BEAM
LINE
d
SLIT
ARRANGEMENT

Fig. 6.3

meter is attached to the rod which drives the slit and is calibrated to indicate the displacement of the slit from beam tube centre with an accuracy of ±1.0 mm i.e. beam displacement 'x'.

The slit positioning assembly is shown in Fig. 6.4 with an inset of the slit face. Measurements taken from the oscilloscope screen result in the emittance shape shown in Fig. 6.5. The horizontal emittance of the cyclotron at 28 MeV is the area enclosed by the contour i.e. 75 mm-mrad.

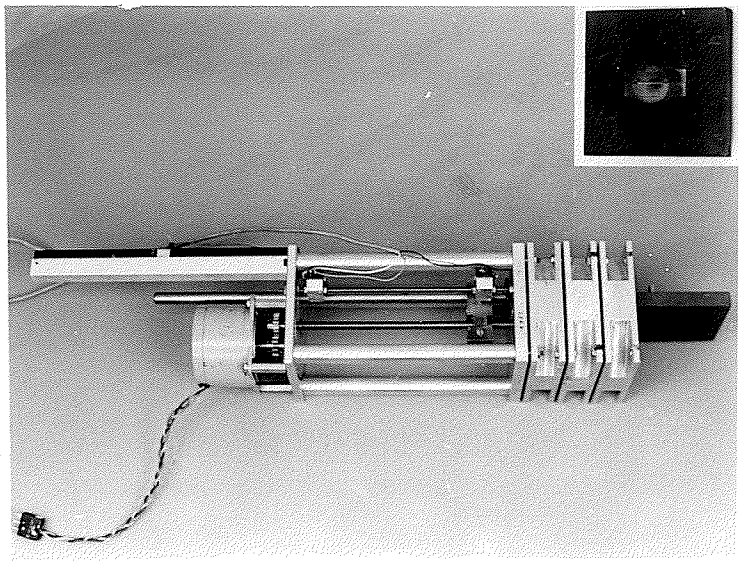

Fig. 6.4 Slit positioning Assembly.

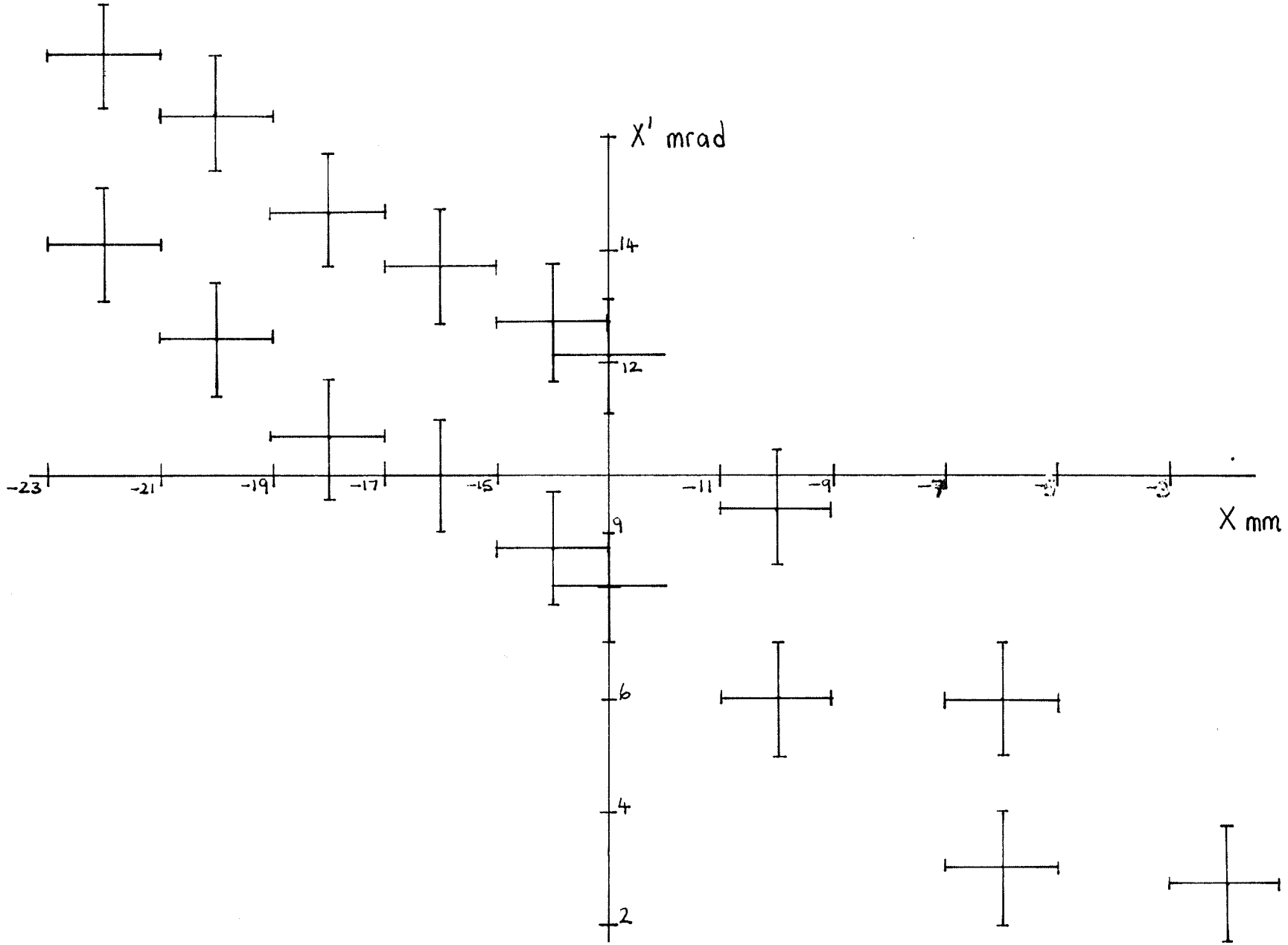

Fig 6.5 Emittance plot for 28MeV proton beam. The area enclosed by the contour is ~75 mmmrad.

III. COMPUTER INTERFACING

The slit and scanner arrangement were interfaced to the cyclotron PDP-15 computer to give a computer controlled emittance measurement device. After moving the slit the computer reads the output from the beam scanner, computes the maximum and minimum angular divergences and plots the resulting points on a CRT display. The computer then moves the slit to a new position and repeats the process. The maximum and minimum displacements of the slit desired are entered into the program before the process begins. At the end of the run the complete emittance shape is shown on the CRT display and the emittance shape can be plotted by the computer if desired.

The computer interface works by relating time intervals to the displacement of a beam profile. The process is shown in Fig. 6.6 three time intervals are measured:

1. The time for a complete scan (T_1)
2. The time from the start of the scan to the first detected beam (T_2)
3. The time from the start of a scan to the end of the beam profile (T_3)

Each of these three intervals gates a 10 MHz oscillator to three CAMAC scalers, as each interval ends the count in each scaler will be proportional to the respective time interval. Circuit details of the interface are given in Fig. 6.7.

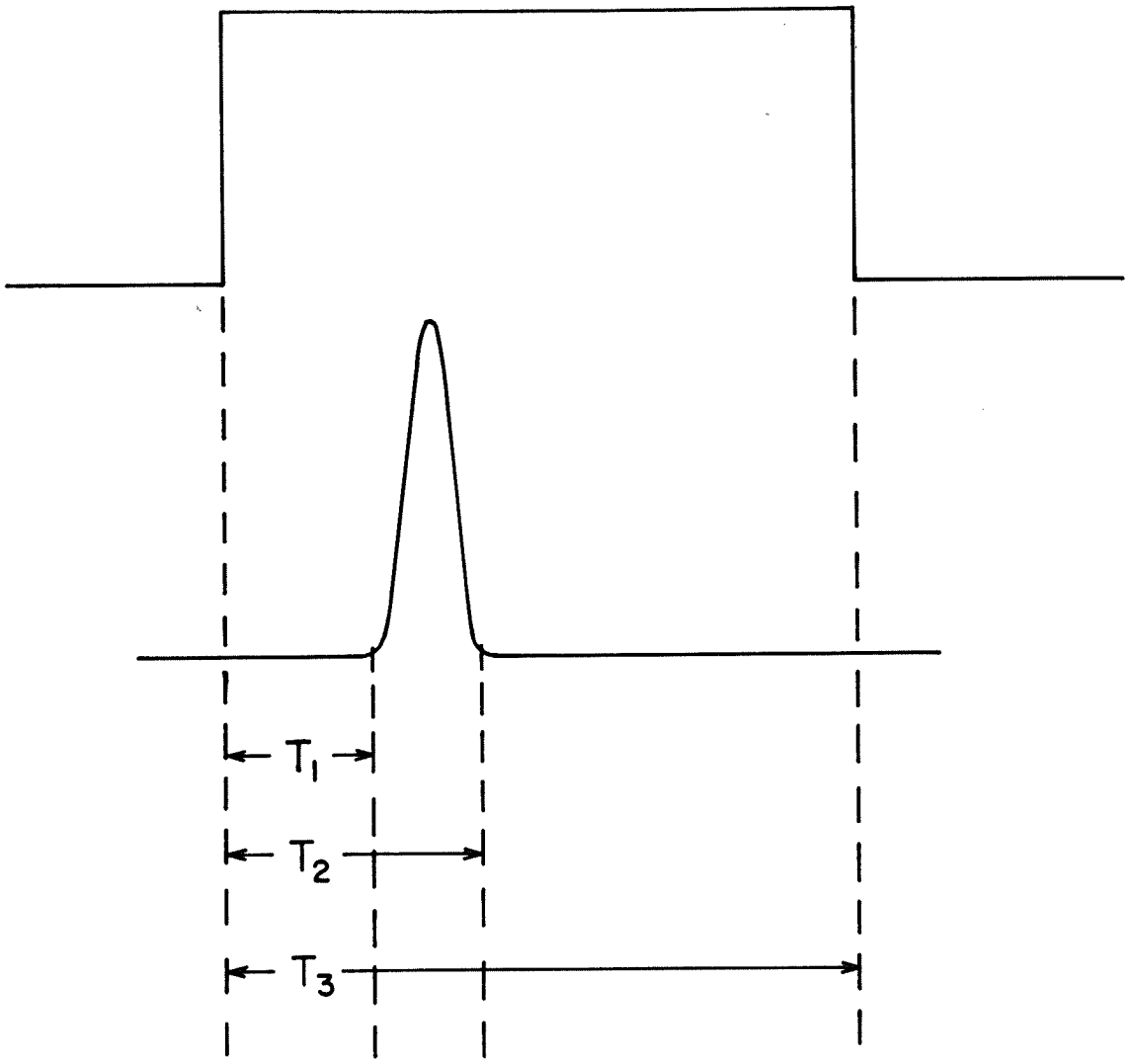

Fig. 6.6

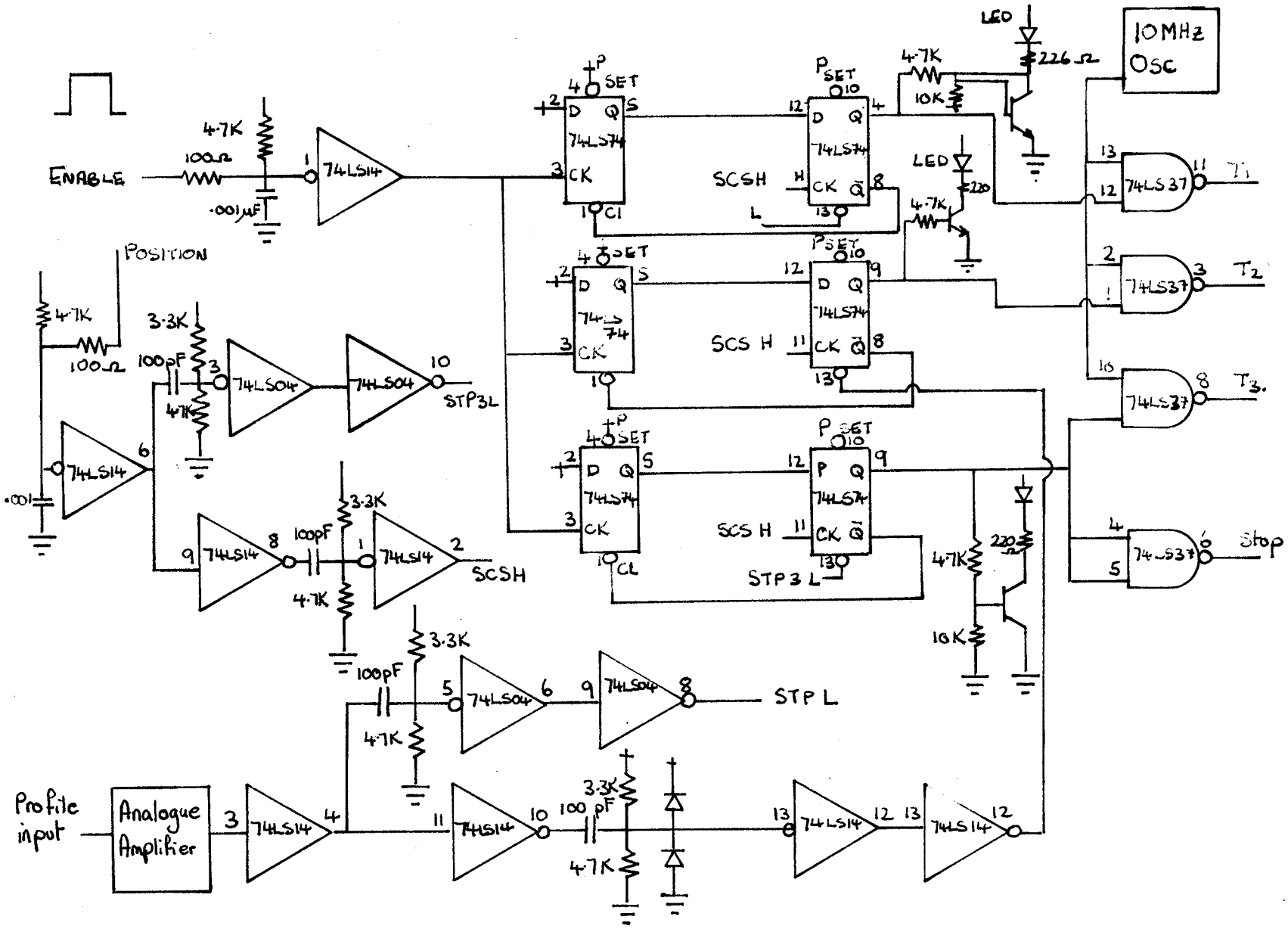

Fig. 6.7 Beam Scanner - computer interface details.

Since the time T_3 corresponds to 6.3 cm i.e. the diameter of the rotating arm on the scanner, the position of the beam can be determined by taking the ratio of T_1 to T_2 to T_3 this also eliminates any problems which may occur with a varying motor speed.

The slit position is read into the computer by connecting the precision potentiometer output to a CAMAC ADC. Two positions of the slit are entered into the computer which reads the ADC at each position. The slit movement is calibrated from these two points as there is a linear relation between slit position and potentiometer output. This feature is used only once when the emittance of the cyclotron is to be measured but is useful when the emittance measuring device is used elsewhere in the accelerator structure.

In operation the computer program clears the scalers, positions the slit and then enables the interface. The leading edge of the square wave output from the scanner starts all three times intervals which end at the appropriate times described above. The program then reads the scalers, calculates the position of the beam profile and prints out the values of displacement (x) and angular divergences (θ_1 and θ_2). Data points are plotted on a CRT screen and at the end of the process the emittance value is printed out. A correction in the computer program takes into account that the wire moves on a circumference of a circle. A complete scan takes approximately 30 seconds depending on the number of readings the program is told to take.

CONCLUDING REMARKS

A beam scanner was designed and built at the University of Manitoba cyclotron facility. The scanner could detect an 18 nano-Ampere 28 MeV beam from the cyclotron exit port and currents as low as a few hundred pico-Amperes in the ion source hall.

The scanner was used in conjunction with a moveable slit to measure emittances at various locations in the accelerator structure.

Further work would involve improving the resolution of the scanner at the high energies and this could be done via analogue to digital conversion of the beam profile output. For very low beam currents at energies of 50 MeV a stepping motor scanner which steps through the beam in such a way that the random and periodic noise that limits the device can be removed is being considered.

REFERENCES

1. K. Johnson and W.J. Ramler, International Conference on Sector-focused Cyclotrons and Meson Factories, April, 1963.
2. D. Reagan, Rev. Sci. Instrum. 37 (1966) 1190-1191.
3. Shigeru Okabe, et al, Rev. Sci. Instrum. 41 (1970) 1537-1539.
4. L.G. Hyman and D. Jankowski, Nucl. Instrum. Meth. 113 (1973) 285-286.
5. S. Miono, Nucl. Instrum. Meth. 128 (1975) 173-174.
6. H. Piceni and C. DeVries, Nucl. Instrum. Meth. 51 (1967) 87-92.
7. C.K. Hargrove and J.P. Legault, Nucl. Instrum. Meth. 113 (1973) 141-145.
8. A McIlwain, Nucl. Instr. and Meth. 136 (1976) 511.
9. J. Takacs, IEEE Trans. Nucl. Sci. (June, 1965) 980.
10. J.W. Jagger, et al, Nucl. Instrum. and Meth. 49 (1967) 121.
11. I.A. Prudnikov, et al, Nucl. Instrum. and Meth. 114 (1974) 101-104.
12. R.J. Vader and O.C. Dermas, Nucl. Instrum. and Meth. 114 (1977) 423.
13. H.P. Beck and R. Langkau, Zeitschrift für Natuforschung A 30 (1975) 981.

14. E.J. Sternglass, Phys. Rev. 108 (1957) 1-12.

15. E.J. Sternglass, Phys. Rev. 93 (1954) 929

16. Hill, Beuchner, Clark and Fisk, Phys. Rev. 55 (1939) 463.

17. "Principles of Cyclic Particle Accelerators", J.J. Livingwood, Chapter 15 Van Nostrand 1961.

18. D.L. Judd, Ann. Rev. Nucl. Sci. 8 181 (1958).

19. Transport of Charged Particle Beams, (A.P. Banford. E. F. Spon) Chapter 2 (1966).